Constraints on the early delivery and fractionation of Earth's major volatiles from C/H, C/N, and C/S ratios

Marc M. Hirschmann Dept. of Earth Sciences, University of Minnesota, Minneapolis, MN 55455 USA *mmh@umn.edu*

Revised for American Mineralogist

Abstract

Earth's inventory of principle volatiles C, H, N, and S, is a legacy of its early stages of accretion and differentiation. Elemental ratios (C/H, C/N, C/S) are powerful tools for understanding early processing of Earth's volatiles, as they monitor relative fractionations through important processes even when absolute concentrations are less-well defined. The C/H ratio of the bulk silicate Earth (BSE), defined from surface reservoirs and minimally degassed oceanic basalts is 1.3±0.3, which is 5-15 X lower than the C/H ratio of carbonaceous and enstatite chondrites and 2-5 X lower than ordinary chondrites. The BSE C/N ratio is superchondritic (40±8; Bergin et al. 2015) whilst the C/S ratio (0.49±0.14) is nearly chondritic. Successful models of volatile acquisition and processing must account for the effects of accretion, core formation, and atmospheric loss on all three of these ratios.

Simple models of equilibration between a magma ocean, the overlying atmosphere, and alloy destined for the core are used to explore the influence of core formation and atmospheric loss on major volatile concentrations and ratios. Among major volatile elements, C is most siderophile, and consequently core formation leaves behind a non-metallic Earth with low C/H, C/N, and C/S ratios compared to originally accreted materials and compared to the BSE. Compared to the predicted effect of early differentiation, the relatively high C/X ratios of the BSE argue in part

This is a preprint, the final version is subject to change, of the American Mineralogist (MSA)
Cite as Authors (Year) Title. American Mineralogist, in press.
(DOI will not work until issue is live.) DOI: http://dx.doi.org/10.2138/am-2016-5452

that significant volatile replenishment occurred after core formation ceased, possibly in the form of a late veneer. However, a late veneer with chondritic composition is insufficient to explain the pattern of major volatile enrichments and depletions because BSE C/H and C/N ratios are non-chondritic. The C/H ratio is best explained if an appreciable fraction of H in the BSE predates delivery in the late veneer. Although atmospheric blow-off is an attractive explanation for the high C/N ratio, available data for C and N solubility and metal/silicate partitioning suggest that atmospheric blow-off cannot counter core formation to produce subchondritic C/N. Thus, unless virtually all core-forming metal segregated prior to volatile accretion (or relative C and N solubilities are appreciably different from those assumed here), the BSE C/N ratio suggests that accreting materials had elevated ratios compared to carbonaceous chondrites. One possibility is that a fraction of Earth's volatiles accreted from differentiated C-rich planetesimals similar to the ureilite parent body. Reconciling C/H, C/N, and C/S ratios of the BSE simultaneously presents a major challenge that almost certainly involves a combination of parent body processing, core formation, catastrophic atmospheric loss, and partial replenishment by a late veneer. The chondritic C/S ratio of the BSE and relatively low S content of the BSE constrains the BSE C concentration, but a potential complicating factor in interpreting the BSE C/S ratio is the possible effect of segregation of an S-rich matte to the core during the later parts of core-mantle differentiation.

INTRODUCTION

The inventory of major volatile elements, hydrogen, carbon, nitrogen, and sulfur, in the bulk silicate Earth (BSE) is one of the distinguishing features of our planet. The storage and fluxes of each of these elements in and between Earth's principal reservoirs, the mantle, crust, and fluid

envelopes, constitute deep Earth volatile cycles which influence the dynamics and history of the planet's geology, climate, and habitability (McGovern and Schubert, 1989; Sleep and Zahnle, 2001; Hayes and Waldbauer, 2006). The masses of these elements present today in Earth's mantle and surface reservoirs are in part a product of the early history of the Earth, including the accretion of different volatile-rich materials and their fate during primary planetary differentiation.

Understanding the delivery, retention and loss of volatiles to growing terrestrial planets, as well as their storage in the primitive core, mantle or magma ocean, and atmosphere is a significant challenge, requiring experimental constraints on solubilities and partitioning and appropriate theoretical understanding of the processes of accretion, differentiation, and impact-related mass erosion. Observational constraints include volatile concentrations (as well as isotopic ratios) in the modern BSE and in plausible cosmochemical sources as represented today by meteorites and comets (Marty, 2012; Halliday, 2013; Bergin et al., 2015). Absolute concentrations in relevant reservoirs are not easily constrained – in particular for N and C, for which estimates of mantle concentrations come chiefly from partially degassed basalts (Marty and Zimmerman, 1999; Cartigny et al. 2001; 2008; Saal et al. 2002). For this reason, ratios of major volatiles, such as C/H and C/N, are most powerful tools for comparison between cosmochemical sources and modern terrestrial reservoirs (Kuramoto, 1997; Hirschmann and Dasgupta, 2009; Marty, 2012; Halliday, 2013; Bergin et al., 2015).

Ratios of major volatiles also provide considerable insight because the comparative behavior of elements through particular processes facilitates hypothesis testing. For example, the low C/H ratio of the BSE relative to plausible chondritic sources (Hirschmann and Dasgupta, 2009) is not consistent with simple origin of Earth's principle volatiles by accretion of late-arriving volatile-

rich planetesimals (e.g. Albarède, 2009; Albarède et al. 2013). The C/N ratio of the BSE is also potentially instructive, though its significance is debated. Marty (2012) and Roskosz et al. (2013) suggested that the N depletion evident in the BSE compared to chondrites could be owing to sequestration in the core, but Chi et al. (2014), Tucker and Mukhopadhyay (2014) and Bergin et al. (2015), noting that C is more siderophile than N, argued that the high C/N ratio of the BSE cannot be owing to core capture. Tucker and Mukhopadhyay (2014) and Bergin et al. (2015) suggested that this key ratio may be more consistent with massive atmospheric blow-off, as N is less soluble than C in magmas and therefore should have been enriched in early atmospheres degassed from a largely molten Earth.

Even if core formation cannot account for specific major volatile ratios of the BSE, such as C/N, removal of metal should have had a profound effect on Earth's volatile budget because all four (H,C,N, and S) are siderophile (Okuchi, 1997; Dasgupta and Walker, 2008; Roskosz et al. 2013; Boujibar et al. 2014) and so their BSE inventory is in part a remnant of the fraction that did not segregate to the core. The most extreme case may be C, for which the very large alloy/silicate partition coefficient led Dasgupta et al (2013) and Chi et al (2014) to conclude that core formation leaves behind a planet effectively devoid of C, and that the BSE carbon inventory derives chiefly from a late veneer delivered after segregation of metal to the core had effectively ceased.

An important consideration that has been ignored during some analyses of segregation of volatiles from a magma ocean to the core is that the concentrations of volatiles in magma oceans are influenced by their solubilities. This means that the atmosphere overlying a magma ocean can be an important reservoir of major volatiles (Kuramoto and Matsui, 1996; Hirschmann, 2012), and particularly so for C and N, which are comparatively insoluble. Thus, in contrast to

This is a preprint, the final version is subject to change, of the American Mineralogist (MSA)
Cite as Authors (Year) Title. American Mineralogist, in press.
(DOI will not work until issue is live.) DOI: http://dx.doi.org/10.2138/am-2016-5452

refractory siderophile elements, constraints on alloy/silicate partition coefficients are insufficient to quantify the effect of core formation on BSE (silicate+atmosphere) major volatiles (Fig. 1).

In this contribution, we review known constraints on major volatile ratios in the BSE compared to relevant cosmochemical sources. In addition to C/H and C/N ratios, previously discussed by others (Kuramoto and Matsui, 1996; Hirschmann and Dasgupta, 2009; Marty, 2012; Roskosz et al 2013; Halliday 2013; Chi et al 2014; Tucker and Mukhopadhyay, 2014; Bergin et al., 2015), we also consider the C/S ratio, which provides additional constraints on the acquisition and fate of Earths major volatiles. We emphasize that plausible models for major element volatile delivery and processing in the early Earth need to produce terrestrial inventories that are consistent with all the major volatile ratios.

We also develop a simple mass balance model for partitioning of volatiles between magma ocean, core-forming alloy, and overlying atmosphere and consider the influence of variations in solubility on core sequestration of volatiles. The model is not intended to be realistic or comprehensive, but illuminates some of the challenges in understanding the origin of Earth's major volatiles and the constraints that BSE concentration ratios (C/H, C/N, and C/S) place on their accretion and loss during early formation and differentiation of terrestrial planets.

TERRESTRIAL AND COSMOCHEMICAL MAJOR VOLATILE RATIOS

C/H

The BSE C/H ratio was considered in detail by Hirschmann and Dasgupta (2009), based on inventories in surficial reservoirs and C/H ratios of undegassed or minimally degassed basalts. (The original analysis considered H/C ratios, which we invert in order to be consistent with the C/N and C/S ratios discussed in this paper). Their analysis showed that the depleted mantle and

OIB source regions appear to have C/H mass ratios of approximately 1.3±0.3 and 2±0.5, respectively. Combined with the H-enriched surface reservoir (C/H=0.5), they inferred that the BSE C/H is 1±0.4. Considerable new data for oceanic basalts have become available since the publication of Hirschmann and Dasgupta (2009) (Fig. 2). As discussed by Hirschmann and Dasgupta (2009), that translation of CO_2 and H_2O analyses of possibly undegassed basalts to C/H ratios in mantle reservoirs requires interpretation. Interfering effects include fractionation of C and H during partial melting and degassing, analytical artifacts giving spurious C concentrations in glasses, and diffusive loss of H from melt inclusions (Hirschmann and Dasgupta, 2009; Gaetani et al. 2012; Rosenthal et al., 2015). Objective adjustments for these effects is not always possible. With that caveat, the data summarized in Fig. 2 are mostly consistent with the analysis of Hirschmann and Dasgupta (2009), but with somewhat higher C/H ratios: 1.55±0.35 for the depleted mantle and 2.2±0.3 for average OIB source regions.

Based on these mantle C/H ratios, the BSE C/H ratio can be estimated from a Monte Carlo simulation similar to that performed by Hirschmann and Dasgupta (2009) to be 1.13±0.20 if it is assumed that the MORB-source comprises 30-80% of the mantle (Workman and Hart, 2005; Arevalo et al., 2009) and that the MORB and OIB sources contain, respectively, 120±40 and 500±200 ppm H_2O. This range of H_2O contents is similar to, but slightly more restricted than that advocated from the review of Hirschmann (2006) (125±75 ppm for MORB source, 650±350 ppm for the OIB source, For the BSE estimate, surface reservoir masses are taken from Hirschmann and Dasgupta (2009). For H and C, the consequent mantle concentrations of H and C are 32±12 and 66±29 ppm, respectively, and BSE masses are 3.1±0.5 X 10^{23} g and 3.6±1.1 X 10^{23} g.

An alternative strategy for constraining mantle C/H ratio is to estimate the C concentration based on C/Nb and C/Ba ratios of possibly undegassed basalts. Rosenthal et al. (2015) combined observations from basalts with experimentally-determined partition coefficients for C, Nb, and Ba to estimate that the MORB and OIB sources contain, respectively, 75±25 and 600±200 ppm CO_2 (20±7 and 165±55 ppm C). Employing the same H concentrations and possible fractions of MORB and OIB source as above, this corresponds to bulk mantle C concentration of 85±33 ppm a BSE C/H ratio of 1.4±0.4

Chondrites (Kerridge, 1985; Jarosewich, 2006; Schaefer and Fegley, 2007) have high C/H ratios compared to the BSE (Fig. 3), though accurate determinations of precise H contents of meteorites requires care, owing to the interfering effects of terrestrial H_2O contamination. Such problems are minimized by considering only meteorite falls, which have suffered less terrestrial weathering than finds. For example, in the compilation of Jarosewich (2006), the average C/H of H ordinary chondrite falls is 1.8 (n=27), but for finds it is 0.5 (n=23). Also, step heating experiments show that the H_2O liberated from chondrites at low temperature is isotopically light and comparable to terrestrial water (Robert and Epstein, 2002), and so studies in which these are not distinguished (e.g., Robert, 2003) are avoided in the compilation. Therefore Fig. 3 considers only falls, and shows that carbonaceous and enstatite chondrites have C/H 5-15 times greater than BSE and ordinary chondrites 2-5X greater. Comets are seemingly unlikely sources of significant terrestrial H and other major volatiles, owing to strong differences in H and N isotopes (e.g., Marty, 2012; Altwegg et al., 2015). The subchondritic BSE C/H ratio remains a key observation that must be explained by any viable history of earth's volatile accretion and loss.

C/N

159 The C/N ratio of the BSE has received considerable recent attention (Roskosz et al. 2013; Tucker
160 and Mukhopadhyay, 2014; Chi et al., 2014; Bergin et al., 2015) because it is greater than those of
161 CI chondrites, the class of carbonaceous chondrites most commonly compared to bulk Earth
162 compositions (Marty, 2012: Halliday, 2013), but the actual ratio remains the subject of
163 controversy. Marty (2012) estimated a C/N mass ratio of 313, whilst in contrast Halliday's
164 (2013) preferred ("basalt") model amounts to 39, or a factor of 8 lower. Earth's surface
165 reservoirs have a low C/N ratio (15, Bergin et al., 2015) and that in the mantle is greater (e.g.
166 713, according to Marty and Zimmerman, 1999), so the discrepancy derives in large part from
167 differences in the total mass of C in the mantle inferred by each model, with consequently
168 greater or lesser influences of surface versus mantle reservoirs on the BSE C/N ratio. The
169 models of Marty (2012) and Halliday (2013) have 766 and 45 ppm mantle C, respectively (788
170 and 67 ppm for the BSE), and so the BSE C/N ratio is more similar to the mantle in the former
171 and more similar to the surface in the latter.

172 Recently, Bergin et al. (2015) estimated the BSE C/N mass ratio to be 40±8. Their method
173 calculates mantle C concentration from CO_2/Nb and CO_2/Ba ratios of oceanic basalts, exactly as
174 described in the previous section. It uses the surface mass of N (6.4±1.1 X 10^{21} g) from Goldblatt
175 et al. (2009) and a mean mantle N concentration of 1.1±0.55 ppm from the N/Ar ratios of basalts
176 (174±56 for MORB; 105±35 for OIB, Marty and Dauphas, 2003), together with estimates from
177 bulk mantle Ar concentration deriving from whole-Earth K-Ar budgets (McDonough and Sun,
178 1995; Arevalo et al. 2009). This approach is similar to that of Marty (2012) and relies on the
179 empirical observation that N/Ar ratios of basaltic glasses and their vesicles do not vary
180 significantly, owing to similar solubilities during low pressure degassing (Cartigny et al. 2001).

The inferred BSE C/N ratio is significantly greater than those measured from CI chondrites (Fig. 4). Other volatile rich carbonaceous chondrites, including the CM, and CR classes, also have C/N ratios <25. The situation for volatile-depleted CO and CV chondrites is, however, less clear, in part because different studies indicate strikingly different C/N ratios (Fig. 4). Most CO and CV meteorites analyzed by Pearson et al (2006) and Alexander et al. (2012) yield low C/N ratios similar to CI, CM, and CR chondrites, but some are not so different from the BSE and the averages of CO and CV meteorites analyzed of Kerridge (1985) indicate much greater C/N ratios. For particular CO and CV stones analyzed in the different studies, Kerridge (1985) reports significantly less N, resulting in high C/N. This suggests that discrepancies between studies are partly owing to different analytical techniques, accuracies, or procedural blanks. More work is required to establish which values best portray the diversity of C/N ratios in carbonaceous chondrites.

Also shown on Fig. 4 are compositions of enstatite and ordinary chondrites. The former have very low C/N ratios (Grady et al. 1986; Wasson and Kallemeyn, 1988), below those of carbonaceous chondrites, but ordinary chondrites (Schaefer and Fegley, 2007; Bergin et al. 2015) have a wide span of C/N ratios, including those that reach and far exceed those of the BSE. The great variability among ordinary chondrites is in part owing to low concentrations of both C and N, with high uncertainties near limits of detection.

In summary, the BSE C/N ratio is high compared to CI chondrites, but similar to or even lower than ratios spanned by other classes of meteorites, including possibly carbonaceous (CV, CO) and ordinary chondrites. Compared to primitive CI chondrites, these have undergone more significant parent body processing which has lead to preferential N loss and thereby increased C/N ratios.

This is a preprint, the final version is subject to change, of the American Mineralogist (MSA)
Cite as Authors (Year) Title. American Mineralogist, in press.
(DOI will not work until issue is live.) DOI: http://dx.doi.org/10.2138/am-2016-5452

204 **C/S**

205 To construct the C/S ratio of the BSE (Fig. 5), we adopt a BSE S content of 225±25 ppm,
206 consistent with estimates of Morgan (1986) (200 ppm); McDonough and Sun (1995) (250±50
207 ppm), and Wang and Becker (2013) (211±40 ppm), which derive chiefly from peridotite
208 compositions. It is higher than estimates derived from S/Dy ratios of basalts: e.g., 146±35 ppm
209 for the Siqueiros MORB source (Saal et al. 2002) or 119±30 ppm for the depleted mantle
210 (Salters and Stracke, 2004), but the controls on S/Dy ratios in MORB, including f_{O2}, sulfide
211 fractionation, and major element melt composition, have been little-explored and so the estimates
212 from peridotites seem more robust. For carbon we adopt the procedure based on C/Nb and C/Ba
213 ratios described in the section on C/H ratios. Inventories of S in the continental and oceanic
214 crust, and storage of S in sea floor sediments or evaporates, are ~1% of the mantle mass (e.g.
215 Canfield, 2004), and therefore do not affect the BSE S inventory within uncertainty. With
216 uncertainties calculated from a Monte Carlo simulation, the resulting C/S mass ratio of the BSE
217 is 0.49±0.14.

218 C/S for different classes of meteorites (Fig. 5) are derived from the average compositions
219 cataloged by Wasson and Kallemeyn (1988). CM and CI carbonaceous chondrites have C/S
220 ratios (0.67 and 0.55, respectively) similar to the BSE, whilst ratios of other classes of
221 carbonaceous, ordinary, and enstatite chondrites are distinctly lower (≤0.25). Thus, the BSE C/S
222 ratio is within the range recorded by carbonaceous chondrites and greater than that for ordinary
223 and enstatite chondrites.

224 **Summary of BSE major volatile element fractionations**

225 The salient features of the BSE major volatile inventory, summarized in Table 1, are (1) the C/H
226 ratio is subchondritic, (2) the C/N ratio is higher than volatile-rich classes of carbonaceous

chondrites and than enstatite chondrites, but volatile-poor carbonaceous chondrites and ordinary chondrites have highly variable ratios that may be as great or greater than the BSE, and (3) the C/S ratio is similar to that of carbonaceous chondrites and greater than that of ordinary and enstatite chondrites. These specific characteristics are clues to the origin and history of BSE's major volatiles. They reflect the combination of volatile sources and the processes of differentiation and loss during Earth's early assembly.

SIMPLE MODELS OF CORE FORMATION AND ATMOSPHERIC LOSS

Volatiles delivered to the accreting planet were potentially lost to space or sequestered in the core. Thus, the BSE volatile inventory represents the mass accreted that avoided core formation and atmospheric blow off. The magnitude of such losses are related to the timing of accretion relative to the processes of core segregation and impact-induced loss, as well as to the partitioning of the volatiles between silicate, metal, and vapor.

A simple model to explore the processing of major volatiles between the principal early Earth reservoirs is to consider a magma ocean overlain by an atmosphere and equilibrating with some fraction of metal that is destined for the core (Fig. 1). A key feature of this type of model, considered previously by Kuramoto and Matsui (1996), Hirschmann (2012), and Bergin et al. (2015) is that the concentration of a volatile dissolved in the magma ocean is determined by its solubility imposed by the vapor pressure of the overlying atmosphere, which in turn is calculated from the mass of the atmosphere. The magma ocean also equilibrates with a fraction of core-destined metal as it transits the molten mantle during accretion (Dahl and Stevenson, 2010; Deguen et al. 2014; Wacheul et al. 2014). Metal/silicate partitioning occurs between volatiles in the magma ocean and the fraction of metal equilibrating during delivery to the core, which can be less than the total mass of the core because (a) as much as half of the metal arrives early in the

This is a preprint, the final version is subject to change, of the American Mineralogist (MSA)
Cite as Authors (Year) Title. American Mineralogist, in press.
(DOI will not work until issue is live.) DOI: http://dx.doi.org/10.2138/am-2016-5452

accretion history, before appreciable volatiles have been delivered (e.g., Raymond et al. 2007; O'Brien et al. 2014) and (b) some portion of the accreting metal could pass through the magma ocean without fully equilibrating with the magma, depending on the length scale of the transiting metal domains or droplets (Dahl and Stevenson, 2010; Deguen et al. 2014; Wacheul et al. 2014, Rubie et al. 2015).

In this simple model, the total mass M_i of a volatile component *i* is given by mass balance:

$$M_i = M_i^{silicate} + M_i^{alloy} + M_i^{atmosphere} . \quad (1)$$

and the concentration in the silicate and the metal, $C_i^{silicate}$ and C_i^{alloy}, are given by

$$C_i^{silicate} = M_i^{silicate} / m^{silicate}; \; C_i^{alloy} = M_i^{alloy} / m^{alloy} \quad (2a, 2b)$$

where $m^{silicate}$ and m^{alloy} are, respectively the mass of the magma ocean and the total mass of all the alloy equilibrating with the magma ocean. Note that the mass of metal is assumed to be in equilibrium with the entire magma ocean. Thus any time-dependent effects of Rayleigh fractionation or competition between volatile delivery and core sequestration are neglected. Equilibrium between silicate and alloy is given by a simple partition coefficient

$$D_i^{alloy/silicate} = C_i^{alloy} / C_i^{silicate}, \quad (3)$$

and the mass of a vapor species in the atmosphere is related to the vapor partial pressure, P_i, by

$$P_i = rM_i^{atmosphere} g / A, \quad (4)$$

where *g* is the gravitational acceleration (9.8 m/s^2), *A* is the surface area of the planet (5.1 X 10^{14} m^2) and *r* is the mass ratio between the volatile species and the element of interest (e.g., *r* = 18/2

This is a preprint, the final version is subject to change, of the American Mineralogist (MSA)
Cite as Authors (Year) Title. American Mineralogist, in press.
(DOI will not work until issue is live.) DOI: http://dx.doi.org/10.2138/am-2016-5452

for H_2O vapor, but unity for H_2 vapor). Equilibrium between the atmosphere and the underlying silicate is given by a solubility law

$$C_i^{silicate} = f(P_i), \quad (5)$$

which in many cases can be approximated by a Henrian constant, S_i,

$$C_i^{silicate} = S_i P_i. \quad (6)$$

For the Henrian approximation, combining Equations 1, 2a, 2b, 3, 4 and 6 gives

$$M_i^{atmosphere} = \frac{M_i}{(S_i g / A)(m^{alloy} D_i^{alloy/silicate}) + 1}. \quad (7)$$

This simple model allows evaluation of the propensity of major volatiles to be stored in the core, magma ocean and atmosphere of the nascent Earth, and hence gives some indication of the planetary fractionation of volatiles during core formation and atmospheric blow off.

Alloy/silicate partitioning of major volatiles

Experimental investigations of partitioning of H, C, N and S between molten Fe-rich alloy and silicate melt indicate that all major volatiles are siderophile, meaning that alloy/silicate partition coefficients, $D_i^{alloy/silicate}$ are greater than unity and that the relative preference for alloy increases in the order $D_H^{alloy/silicate} \approx D_N^{alloy/silicate} < D_S^{alloy/silicate} < D_C^{alloy/silicate}$ (Okuchi, 2007; Dasgupta et al., 2013; Boujibar et al. 2014; Chi et al. 2014; Stanley et al. 2014; Roskosz et al. 2013; Armstrong al., 2015). However, available experimental constraints vary for each element. They are extensive for S, which has been studied numerous times (see recent review by Boujibar et al. 2014), whilst for H they are limited to a single study (Okuchi, 1997) owing to extreme

This is a preprint, the final version is subject to change, of the American Mineralogist (MSA)
Cite as Authors (Year) Title. American Mineralogist, in press.
(DOI will not work until issue is live.) DOI: http://dx.doi.org/10.2138/am-2016-5452

experimental challenges created as H_2 exsolves from molten metal during quench. C and N partitioning have been the subject of several recent studies (C: Dasgupta et al., 2013; Chi et al., 2014; Stanley et al., 2014; Armstrong et al. 2015; N: Kadik et al. 2011; Roskosz et al. 2013). For S, and C, metal/silicate partitioning varies significantly with temperature, pressure, oxygen fugacity and melt composition, and values of $D_C^{alloy/silicate}$ and $D_S^{alloy/silicate}$ may be large at very high pressure (but are diminished by high temperatures that might prevail in a deep magma ocean), but at any particular set of conditions, $D_C^{alloy/silicate}$ is apparently always much greater than $D_S^{alloy/silicate}$. For example, calculating of $D_C^{alloy/silicate}$ and $D_S^{alloy/silicate}$ from the parameterizations of Chi et al. (2014) and Boujibar et al. (2014), respectively, along a magma ocean adiabat (Stixrude et al. 2009) at IW-2 yields $D_C^{alloy/silicate}$ / $D_S^{alloy/silicate}$ ratios ranging from 18 at zero pressure up to 900 at 40 GPa. Thus, among major volatiles, C is the most siderophile and should be most affected by core formation. Limited evidence suggests a modest pressure dependence for $D_N^{alloy/silicate}$ (Roskosz et al. 2013), but for H the dependence remains uninvestigated. In the calculations that follow, values of $D_i^{alloy/silicate}$ appropriate for moderate temperatures and pressures are employed (Table 2), as these allow fair comparison between the behavior of the four elements, but we note that values applicable to metal/silicate equilibrium in a deep magma ocean could be more extreme.

An important consideration is the influence of oxygen fugacity on $D_i^{alloy/silicate}$. As C becomes less soluble in silicate melt under more reduced conditions, values of $D_C^{alloy/silicate}$ become larger (Chi et al. 2014; Armstrong et al. 2015). The same may be true for H and the opposite for N, though data are at this time are lacking. Partitioning of S is also f_{O2} sensitive, particularly in

This is a preprint, the final version is subject to change, of the American Mineralogist (MSA)
Cite as Authors (Year) Title. American Mineralogist, in press.
(DOI will not work until issue is live.) DOI: http://dx.doi.org/10.2138/am-2016-5452

regimes where Si or O are important minor components (Boujibar et al. 2014); under plausible core-forming processes, S is less siderophile at more extreme reducing conditions where Si is an important minor component in alloy. Table 2 summarizes the partition coefficients applied in the current models and, though applicable values as a function of temperature, pressure, melt composition and f_{O2} are insufficiently characterized, we emphasize that qualitative conclusions derived from the models are not particularly sensitive to absolute values selected.

Solubilities of major volatiles in silicate melts

The solubility of major volatiles in silicate liquids can be a complex function of melt composition and oxygen fugacity, owing in part to changes in fugacities of volatile vapor components and in speciation of their counterparts in silicate liquids. Magma ocean silicate liquids are likely to be ultramafic, and unfortunately, solubility experiments for such liquids are sparse or unavailable, owing to challenges in quenching glass. Oxygen fugacities may vary during accretion and differentiation, with plausible conditions for alloy-silicate equilibration ranging from IW-3.5 up to IW-0.5 (Javoy et al. 2010; Rubie et al. 2011; Siebert et al. 2013), but, at least towards the end stages of accretion, intermediate conditions close to IW-2 were most likely (Frost et al., 2008). However, the conditions of alloy-silicate reaction may not apply directly to those for magma ocean-atmosphere equilibration, as magma oceans may have vertical redox gradients, such that conditions prevailing at the surface could be either more oxidized or more reduced than those at depth (Hirschmann, 2012). The values employed in model calculations are summarized in Table 2, and discussed in the paragraphs below.

Under oxidizing conditions, C dissolves in mafic or ultramafic silicate liquids as carbonate ion, with solubility for basalts well-constrained by experiment (e.g., Stolper and Holloway, 1988 Pan et al. 1991; Stanley et al. 2011) and greater concentrations observed for more depolymerized

liquids (Brooker et al. 2001). For the relatively modest pressures prevailing in terrestrial planetary atmospheres above magma oceans, solubility can be parameterized with a single Henry's law coefficients that, for CO_2, amounts to 1.6 ppm C/MPa (e.g. Stolper and Holloway, 1988; Pan et al 1991). C solubility diminishes under reducing conditions, once elemental C is stabilized relative to carbonate or CO_2 vapor (Holloway, 1992; Wetzel et al. 2013; Stanley et al. 2014; Chi et al. 2014; Armstrong et al. 2015), becoming dominated by C=O species near IW (Wetzel et al. 2013; Stanley et al. 2014; Armstrong et al. 2015) with a solubility of 0.55 ppm C/MPa near IW-2 (Armstrong et al. 2015). At highly reduced conditions, C solubility becomes very low, close to 0.22 ppm C/MPa, as CO species are no longer stable and sparingly soluble C-H or C-N complexes become the principal species (Wetzel et al. 2013; Ardia et al. 2014; Stanley et al. 2014; Armstrong et al. 2015; Chi et al. 2015).

Hydrogen is highly soluble in silicate liquids, so long as conditions are sufficiently oxidizing to stabilize dissolved magmatic OH^- or H_2O. Under moderately reducing conditions (e.g. IW-2) at low pressure, H_2 becomes the dominant hydrous vapor species, but H_2O (or OH^-) remains the principle magmatic species, and so hydrogen remains highly soluble in magmas (Hirschmann et al. 2012). However, under highly reducing conditions (~IW-3.5), fugacities of H_2O are low, and H dissolves in silicate liquids sparingly as molecular H_2 (Hirschmann et al. 2012) with a Henry's law coefficient of 5 ppm/MPa – though the compositional and temperature dependence remain poorly characterized. Because OH^- solubility is proportional to the square root of H_2O fugacity, the simple Henrian approximation (Eqn. 6) is usually not appropriate for H_2O solubility even for relatively modest H_2O partial pressures. In the calculations below, we use the model of Moore et al. (1998), which suggests a solubility near 4000 ppm/MPa at low pressures (near 100 kPa H_2O

partial pressure) but considerably less for more massive atmospheres (e.g., 400 ppm/MPa for 300 bars H_2O partial pressure).

Under oxidizing conditions, nitrogen occurs in silicate melts chiefly as N_2, which is comparatively insoluble, with a Henrian coefficient of approximately 1 ppm/MPa (Libourel et al. 2003). Under reducing conditions, solubility increases significantly owing to CN^- and/or NH_x ionic species, the latter being important at high pressure, where conditions close to IW are sufficient to stabilize appreciable dissolved N (Libourel et al. 2003; Mysen and Fogel, 2010; Kadik et al. 2011; Roskosz et al. 2013). For conditions near IW-2, N solubility is poorly constrained and likely depends on the ambient H_2 fugacity, but may be close to 5 ppm/MPa (Roskosz et al. 2013). CN^- becomes stable under highly reduced conditions at low pressure producing a solubility in excess of 50 ppm/MPa (Libourel et al. 2003). The relative roles of CN^- and NH_x species under reducing conditions with appreciable H_2 fugacities remain poorly quantified.

Among the major volatiles, S is the most soluble, with concentrations of 10^3-10^4 ppm for sulfur fugacities less of than 0.1 MPa. Specific solubilities are a complex function of melt and gas composition, and increase as conditions become more reducing (O'Neill and Mavrogenes, 2002). Here we adopt a conservative Henrian coefficient of 5000 ppm/MPa S, where the sulfur partial pressure is the sum of all possible sulfurous species (S_2, H_2S, SO_2, etc.). Assuming higher solubilities would not influence any of the conclusions of the modeling.

Model Calculations

To explore a range of plausible conditions applicable to formation of a primitive atmosphere above a magma ocean, we consider 3 characteristic conditions with possibly relevant oxygen fugacities–intermediate (~IW-2), comparatively oxidized (~IW+1), and strongly reduced (IW-

3.5). The intermediate (~IW-2) conditions are similar to conditions thought to be typical of magma/metal equilibration at the end-stages of accretion and differentiation (e.g., Rubie et al. 2011). The oxidized (~IW+1) conditions are not compatible with equilibration with metal, but could apply to silicate-atmosphere equilibration in a deep magma ocean in which conditions might be more oxidized at the surface than at depth (Hirschmann, 2012). The very reduced conditions (IW-3.5) could apply to early stages of terrestrial accretion (Javoy et al. 2010; Rubie et al. 2011), though this was likely prior to the era of principle volatile delivery on Earth (e.g., Jacobson et al. 2014), but also could apply in instances of a shallow magma ocean, where conditions at the surface are more reduced than at depth (Hirschmann, 2012). The solubilities and metal/silicate partition coefficients for each set of conditions are summarized in Table 2.

Each calculation considers equilibration of a molten mantle with a mass of metal ranging from zero to 0.5 the silicate mass. If the entire core equilibrated with the silicate Earth, then 0.5 is the appropriate alloy/silicate ratio, and lower ratios indicate partial equilibration, as would be expected if significant fractions of the core segregated prior to accretion of the bulk of terrestrial volatiles (Jacobson et al. 2014). After equilibration between the silicate, a given fraction of core-forming alloy, and an overlying atmosphere, the non-metallic Earth volatile inventory can be considered as the sum of the silicate and atmospheric masses or, if the atmosphere is lost to space, as the silicate alone.

Model Results

Fig. 6 illustrates the fraction of each volatile contained in alloy or in the atmosphere overlying the silicate magma ocean for each of the 3 conditions explored. Equilibration with metal depletes the silicate earth of major volatiles, reducing storage in the silicate (not shown), but also reducing the mass of the overlying atmosphere. Corresponding volatile element ratios (Fig. 7)

400 are derived both by summing the silicate and atmospheric reservoirs or, for instances where the
401 atmosphere is subsequently lost to space, counting only the volatiles dissolved in silicate. To
402 distinguish from the BSE, which is the reservoir observed today, model calculations of the
403 silicate or silicate+atmosphere reservoirs are termed the "non-metallic Earth".

404 Crucially, no single combination of conditions (oxidized, reduced, very reduced), fraction of
405 metal extracted, and atmospheric loss or retention produces a non-metallic Earth that matches all
406 the volatile ratios of the BSE. Clearly, this is in part because the scenarios investigated are overly
407 simple. Even with these shortcomings, the particular features of each scenario illuminate well
408 the challenges for accounting for all the BSE volatile inventories.

409 All scenarios produce low C/H ratios compared to chondritic materials, with lower ratios
410 produced if a C-rich, H-poor atmosphere is lost, as for the oxidized and reduced cases. For very
411 reduced conditions, the atmosphere is also H-rich (Fig. 6), and so C/H fractionation is
412 minimized. Equilibration with appreciable metal yields non-metallic Earth C/H ratios lower than
413 the BSE. The key observation is that both core formation and atmospheric loss produce a non-
414 metallic Earth that has low C/H compared to the BSE, owing to preferential loss of C.

415 The non-metallic Earth C/N ratio is diminished dramatically by metal segregation for both
416 oxidizing and reducing conditions (Fig. 7). Atmospheric loss diminishes the magnitude of this
417 effect under oxidizing conditions, but cannot prevent the non-metallic Earth's C/N ratio from
418 becoming low compared to the BSE except under the most extreme circumstances of very small
419 fractions of metal equilibration (alloy/silicate<0.02) combined with loss of an oxidized N-rich,
420 C-poor atmosphere (Figs. 6 and 7). Under reduced or highly reduced conditions, where
421 solubility of N in silicate is high and C is low, extremely low C/N ratios in the non-metallic
422 Earth are produced by core formation and made more extreme if that atmosphere is lost to space.

We note however, that solubilities of N and C remain imperfectly defined under reducing conditions and more N-rich atmospheres, and consequent modest increases in non-metallic Earth C/N owing to atmospheric loss, remain possible except under strongly reducing conditions.

C/S ratios of the non-metallic Earth diminish with segregation of metal, owing to preferential partitioning of C into alloy. However, the change in ratio is small, such that the non-metallic Earth C/S remains similar to that of the BSE, so long as the atmosphere is retained. Because a high temperature atmosphere above a magma ocean is rich in C and poor in S, atmospheric loss leaves a ratio that is significantly lower than the BSE. Under very reduced conditions, the very low solubility of C in silicate lowers the C/S ratio of segregating metal, but most of the C not segregating to the core is in the overlying atmosphere, so that atmospheric loss also produces a very low C/S BSE.

DISCUSSION

Major volatile ratios and processing affecting early volatile differentiation

Despite its simplicity, the present model of equilibration between a whole-earth magma ocean, core-forming metal, and an overlying high temperature massive atmosphere suggests the broad effects of core formation and atmospheric loss on major element volatile ratios. Both core segregation and atmospheric blow off would leave a non-metallic Earth with a low C/H ratio compared to accreted material (Fig. 6), consistent with the observation that the BSE has low C/H compared to chondritic compositions (Fig 3). In most scenarios, the resulting low C/H ratio of the non-metallic Earth is more extreme than the BSE, which either suggests that the fraction of alloy equilibrated with silicate was small, that the extreme ratio produced this way was later modulated by a late veneer (as discussed in greater detail below), or that the model employed suffers from oversimplification.

446 As is the case for C/H, the effects of core formation or core formation combined with
447 atmospheric loss causes C/N to diminish, but because the C/N ratio of the BSE is greater than
448 likely chondritic sources (Fig. 4), this presents a challenge. How did the BSE C/N ratio arise
449 from sources with low C/N if early processing further reduced the ratio of the non-metallic
450 Earth? Importantly, though atmospheric loss has the potential to raise C/N, the combination of
451 core formation and atmospheric loss also produces a non-metallic Earth with low C/N. This is
452 because even small amounts of core formation produces C/N vastly lower than the BSE and this
453 effect cannot be reversed by loss of a N-rich atmosphere under plausible circumstances (Fig 6).

454 In the case of C/S, the BSE has a ratio that is similar to chondritic, but the processes of core
455 formation and atmospheric loss both should reduce the ratio, producing a non-metallic Earth with
456 a C/S ratio substantially lower that that which is observed in the BSE. Either additional
457 processes not considered in the simple model are required, or the effects of core formation and
458 atmospheric loss have been erased by addition of a late veneer (see below).

459 The common theme between the C/H, C/N, and C/S ratios is that processing of chondritic
460 material during primary planetary differentiation, and in particular core formation, leaves a non-
461 metallic Earth that is depleted in C compared to the BSE. A partial explanation for this seeming
462 discrepancy is that the Earth could have accreted in part from a source rich in carbon and
463 depleted in other major volatiles. One obvious candidate would be differentiated planetesimals
464 similar to ureilites. Ureilites are characteristically rich in C (2.9±1.6 wt.%, Grady et al. 1985)
465 and have smaller amounts of in H (500-3000 ppm H, Jarosewich, 2006), N (10-30 ppm, Grady et
466 al. 1985; Downes et al. 2015) and S (0.2-0.6 wt. %; Gibson and Yanai, 1979). Warren (2008)
467 argued that explosive volcanism on planetesimals similar to ureilites may be a plausible source
468 of significant portions of the proto-Earth, potentially accounting for many of the distinctive

This is a preprint, the final version is subject to change, of the American Mineralogist (MSA)
Cite as Authors (Year) Title. American Mineralogist, in press.
(DOI will not work until issue is live.) DOI: http://dx.doi.org/10.2138/am-2016-5452

469 terrestrial depleted and non-chondritic trace element features. Additionally, the inventory of C,
470 H, N, and S may have been augmented after the catastrophic differentiation events by addition of
471 a late veneer.

472 **Alternative C-rich BSE scenarios**

473 The major volatile inventories of the mantle in this work derives chiefly from studies of
474 minimally degassed oceanic basalts and are similar to ratios surmised by Hirschmann and
475 Dasgupta (2009) and the preferred "basalt" model of Halliday (2013). But the C/N ratio
476 estimated here is dramatically lower than that based directly or indirectly on global ^{40}Ar mass
477 balance, which predicts much greater mantle and BSE C concentrations. For example, Marty
478 (2012) gives the bulk mantle C concentration as 766±300 ppm, Halliday's "Layered Mantle"
479 model amounts to 645±400 ppm and the upper limit given by Dasgupta and Hirschmann (2010)
480 is 500 ppm. If such high estimates of mantle C are accurate, then many of the inferences in this
481 paper, particularly those for C/N and C/S, are not valid. Estimates for C/H (Dasgupta and
482 Hirschmann, 2009; Marty, 2012; Halliday, 2013, this work) would not be affected because they
483 all rely on C/H ratios from minimally degassed oceanic basalts (Hirschmann and Dasgupta,
484 2009).

485 Because a significant proportion of the mantle is known to be depleted in C, models that call for
486 volatile-rich average mantle require a deep mantle source that is enriched in inverse proportion to
487 the its total volume. For example, Marty (2012) considers a depleted mantle with 20±8 ppm C
488 and a bulk mantle with 765±300 ppm C. If the enriched deep region amounts to the entire lower
489 mantle (75% of the mantle) (Allegre et al 1996) then its C concentration must be 1100±400. If it
490 is an "abyssal" layer amounting to 20% of the mantle (e.g., Arevalo et al. 2009), then it must
491 have 3700±1400 ppm C; and if it is restricted to D", 5% of the mantle (Tolstikhin and Hoffman,

2005), then it must have 15,000±6000 ppm C. Two lines of reasoning raise doubts about the possibility of such extreme C-rich reservoirs in the deep mantle. The first is that the calculation is based on poorly constrained estimates for the C/Ar ratio of the deep mantle, and the second is that there is no petrologic or geochemical evidence for such a region as sampled by OIB.

Deducing the average mantle C content from bulk mantle ^{40}Ar inventory requires an estimate for the C/Ar ratio of the bulk mantle or from its principle reservoirs. The C/Ar ratio for the MORB source has been estimated indirectly through combined C/N and N/Ar or C/He and He/Ar ratios (Marty, 2012; Halliday, 2013). Undegassed C/N, N/Ar or C/Ar ratios of OIB are poorly known, and so values from MORB (e.g Marty and Zimmerman, 1999) have been employed for bulk mantle calculations instead. Marty (2012) also inferred C concentrations from C/He ratios of gases or fluid inclusions from plume localities (Iceland, Hawaii, Reunion, Yellowstone). However, C/N, C/Ar, and C/He ratios of vesicles, volcanogenic vapors, and well gases vary by more than 2 orders of magnitude (Trull et al., 1993; Sedwick et al., 1994; Hilton, 1998; Marty and Zimmerman 1999; Cartigny et al. 2001; Paonita and Martelli, 2007), in part owing to fractionation during degassing, as well as near-surface effects of assimilation and precipitation (Barry et al 2014). Because such fraction is owing to a combination of Rayleigh and kinetic effects (Aubaud et al. 2004; Paonita and Martelli, 2007), reconstruction of pristine ratios is problematic.

If accurate estimates of C/Ar or C/He ratios of oceanic basalt source regions could be made, they would be applicable to deep volatile source regions only if the former have values characteristic of the putative C-enriched deep mantle. In that case, the C-enrichment should also be expressed in ratios to incompatible trace elements, e.g., CO_2/Nb and CO_2/Ba, in undegassed magmas. Like volatile elements, estimates of the enrichment of incompatible trace elements in deep enriched

This is a preprint, the final version is subject to change, of the American Mineralogist (MSA)
Cite as Authors (Year) Title. American Mineralogist, in press.
(DOI will not work until issue is live.) DOI: http://dx.doi.org/10.2138/am-2016-5452

mantle are inversely proportional to the aggregate volume of enriched mantle, as the depleted mantle (Workman and Hart, 2005) and continental crust (Rudnick and Gao, 2003) have too little Nb and Ba to account for the bulk silicate Earth inventory (McDonough and Sun, 1995). Thus, a bulk mantle with 766±300 ppm C (Marty, 2012) would require an enriched mantle reservoir with CO_2/Nb and CO_2/Ba ratios of 5000±2000 and 850±350, respectively. These are far in excess of the highest values (CO_2/Nb =1200, CO_2/Ba=120 at North Arch, Hawaii, Dixon et al., 1997) observed from OIB, particularly noting that CO_2/Ba ratios of basalts are more faithful recorders of ratios in OIB source regions because of the tendency of CO_2 and Nb to fractionate from one another during small degree partial melting (Rosenthal et al. 2015). To generate typical parental OIB with such high ratios and Ba and Nb concentrations ~100 times primitive mantle (e.g., Hofmann, 1997) the undegassed melt would have implausibly high (>35 wt.%) CO_2 concentrations. Such extreme CO_2 enrichments, even if nearly totally degassed prior to eruption, are inconsistent with the major element character of OIB (e.g., Dasgupta et al. 2007).

Significance of the BSE C/S ratio

Compared to the BSE C/H and C/N ratios, which have been considered previously (Kuramoto, 1997; Hirschmann and Dasgupta, 2009; Marty, 2012; Halliday, 2013; Roskosz et al. 2013; Chi et al. 2014; Tucker and Mukhopadhyay, 2014; Bergin et al. 2015), the significance for the C/S ratio on early acquisition and processing of volatiles on Earth has received scant attention. The comparatively high C/S ratio of the BSE is a potential constraint on the magnitude of loss of C to space early in Earth history. Impact-induced loss of an early atmosphere (or atmospheres) is an important component of many scenarios of early planetary evolution (Melosh and Vickery, 1989; Ahrens 1993; Genda and Abe, 2005; de Neim et al., 2012; Tucker and Mukhopadhyay, 2014; Schlicting et al. 2015). Magma oceans are capable of creating thick CO_2-rich atmospheres (e.g.,

538 Zahnle et al. 2007; Elkins-Tanton, 2008; Hamano and Genda, 2013) and models of atmospheric
539 blow-off commonly conclude that significant C is lost to space (e.g., Genda and Abe, 2005). For
540 example, Hirschmann and Dasgupta (2009) suggested that such blow-off could be one of the
541 processes responsible for the low C/H ratio of the BSE.

542 However, thick C-rich atmospheres are also expected to be S-poor, and therefore to have very
543 high C/S ratios. This is evident in the calculations presented in Figs. 6 and 7, as a result of
544 greater magmatic solubility of S compared to C. It is also consistent with the composition of low
545 and high temperature atmospheres calculated from degassing of a wide range of meteorite
546 compositions (Hashimoto et al. 2007; Schaefer and Fegley, 2007; 2010), which yield vapor
547 compositions with high C/S ratios (although the high temperature calculations neglect
548 stabilization of S-bearing silicate liquid, and therefore exaggerate S vapor pressures). Loss of
549 such atmospheres to space would diminish the C/S ratio of the non-metallic Earth.

550 Because the C/S ratio of the BSE is similar to that of CI or CM chondrites (Fig. 5), a large
551 decrease in the C/S of the non-metallic Earth owing to atmospheric blow off could have been
552 erased by subsequent addition of a chondritic late veneer, as discussed in greater detail below.
553 But this requires that large-scale loss of C to space terminate before delivery of most of the late
554 veneer. Recent calculations by Schlicting et al. (2015) suggest that the many small late impacts
555 could have ablated a significant fraction of atmospheric volatiles, perhaps associated with the
556 very same events that delivered the late veneer. But owing to the high C/S ratio of any plausible
557 early atmosphere, removal of an appreciable C-rich atmosphere would be expected to remove C
558 in preference to S. Consequently, the nearly chondritic C/S ratio of the BSE indicates that late
559 ablation during or after delivery of the late veneer did not remove large fractions of the Earth's C
560 inventory. This does not preclude that such impacts could have ablated a significant fraction of

561 nitrogen or rare gases, which could have been abundant in a low temperature atmosphere in
562 which much of the C had been fixed in rocks by weathering (Sleep and Zahnle, 2001).

563 **Sulfide liquid segregation to the core** One other consideration is the possible loss of
564 significant S to the core by late segregation of a small amount of a sulfide liquid (O'Neill, 1991;
565 Wood and Halliday, 2005) (but see also contrary views, e.g., Rudge et al. 2010; Ballhaus et al.
566 2013). Because C solubility diminishes with the S content of alloy liquids (Wood, 1993,
567 Dasgupta et al. 2009; Tsuno and Dasgupta, 2015; Zhang and Hirschmann, 2016), they have
568 intrinsically low C/S and their segregation to the core would raise the C/S ratio of the non-
569 metallic Earth. In this case, the nearly chondritic C/S ratio could be owing to a combination of
570 atmospheric loss of C balanced by preferential loss of S to the core during late sulfide liquid
571 segregation. In the absence of sulfide/silicate partitioning data for H and N, it is not clear how
572 such a process could affect C/H and C/N ratios of the non-metallic Earth, but as S-poor metal
573 segregation would greatly reduce these ratios, both H and N would have to be highly soluble in
574 sulfide to account for the high C/N ratio of the BSE.

575 **The BSE C/S ratio and C concentration** The C/S ratio is also a potential constraint on the C
576 content of the BSE. In this work, estimates from C/H and combined C/Nb and C/Ba ratios
577 indicate BSE C concentrations of 90±27 or 108±34 ppm and these yield BSE C/S ratios of
578 0.48±0.16 or 0.45±0.18, respectively (assuming BSE S=225±25 ppm). Much larger estimates of
579 BSE C contents include those of Javoy and Pineau (1991), who favored a mantle concentration
580 of 300 ppm on the basis of popping rocks (equivalent to 320 ppm if the carbon surface reservoir
581 is included) and Marty (2012), who favored a BSE C concentration of 789 ppm; these amount to
582 BSE C/S ratios of 1.4 and 3.5, respectively. Because these estimates for C-rich BSE imply C/S
583 ratios that are superchondritic (compare to Fig. 5), they imply that processes of preferential C

584 accretion or S-loss dominated over preferential C loss by segregation of S-poor alloy to the core
585 or atmospheric loss. They also require that the high C/S ratios produced in this way were not
586 obliterated by a chondritic late veneer. More modest estimates for C concentrations in the BSE
587 do not have these stringent correlative implications.

588 **Importance of a Late Veneer**

589 The segregation of alloy to the core and blow off of massive early atmospheres invariably
590 produce more extreme major volatile (C/H, C/N, and C/S) fractionation than is evident in the
591 BSE, if the volatiles were supplied originally from materials similar to carbonaceous chondrites
592 (Figs. 8A and 8B), and this may be because some fraction of the BSE major volatile inventory
593 was added in a late veneer that post-dates these catastrophic events. On the basis of platinum-
594 group element abundances, ~0.3% of the mass of the Earth was added after segregation of metal
595 to the core had effectively terminated (Walker, 2009), and the influence of such an addition is
596 modeled in Figs. 8C and 8D. Two different late veneer scenarios are examined – in the first
597 (Fig. 8C) the material has the composition of CI chondrite, and in the second, it has the a C-rich
598 composition derived from a 80% ureilite and 20% CI chondrite. The latter is not meant to imply
599 that material from the specific ureilite parent body supplied a significant fractions of Earth's
600 volatiles, but rather is an exploration of the consequences of accretion to Earth of volatiles in part
601 from differentiated planetesimals that underwent segregation of a S-rich core, leaving behind a
602 C-rich mantle (e.g., Warren et al., 2006)

603 Scenarios for the non-metallic Earth that include addition of a late veneer (Figs. 8C and 8D) are
604 much more similar to observed BSE concentrations than those that include only core formation
605 and atmospheric loss (Figs. 8A and 8B). In both the chondritic (Fig. 8C) and C-rich (Fig. 8D)
606 late veneer scenarios, the non-chondritic low C/H ratio of the BSE is qualitatively reproduced, at

607 the same time as the chondritic C/S ratio is reproduced, though the latter is true only for a
608 particular range of equilibrated metal fractions (i.e., near 50% metal equilibrated with the magma
609 ocean, prior to arrival of a CI late veneer, near 10% metal equilibrated prior to a C-rich late
610 veneer). The high C/N ratio of the BSE is also qualitatively matched by addition of a C-rich late
611 veneer if the fraction of equilibrated metal is high (i.e., the C and N concentrations are very low
612 following core formation, such that the relative contribution of C and N added by the late veneer
613 is greater), however, such scenarios also produce superchondritic C/S ratios, which do not match
614 the BSE.

615 These scenarios are not meant to be comprehensive. Other compositions of late veneer and
616 different compositions of volatile-bearing carriers in earlier phases of accretion are plausible.
617 Still, these example calculations illustrate that BSE major volatile ratios (C/H, C/N, C/S) may
618 feasibly be reproduced by a combination of core formation, atmospheric loss, and late addition,
619 particularly if the accreted volatiles come in part from C-rich differentiated planetesimals, rather
620 than more pristine bodies. Differentiated planetesimals may be particularly important in the
621 origin of the superchondritic BSE C/N ratio (e.g., Bergin et al. 2015), as early-earth processing
622 seems to produce strongly subchondritic ratios, and addition of chondrites could only dilute, but
623 not reverse that sense of fractionation. However, matching all 3 ratios simultaneously is not
624 straightforward, and simultaneous consideration of all major volatiles is an important constraint
625 on future more quantitative models.

626 A key point is that both a late veneer and early processing by catastrophic events seem required
627 to explain the major volatile ratios of the bulk silicate Earth. The low C/H, C/N, and C/S ratios
628 resulting from simple models of core formation and atmospheric loss are not compatible with
629 those evident in the BSE, and so some volatiles were added to and/or lost from the Earth after

these catastrophic events. But the combination of low C/H and high C/N of the BSE argues that significant volatiles, and in particular, an appreciable fraction of the H that presently comprises the BSE, was delivered *before* these catastrophic events were complete. This because simple late addition of a chondritic late veneer would not create these non-chondritic ratios (Fig. 8C) and because addition of a C-rich late veneer (Fig. 8D), whilst perhaps creating C/N and C/S ratios similar to the BSE, and possibly diminishing extremely low C/H ratios derived from early events (Fig. 8D), could not create a subchondritic C/H BSE ratio. It is also because later processes do not seem capable of producing the observed BSE fractionations starting either from chondritic (late veneer) ratios or early fractionated ratios. For example, late atmospheric losses owing to the ablative effects of impacts (Schlicting et al. 2015) could preferentially remove C relative to H, but if sufficient C were lost in this way from a chondritic source to make the BSE low in C/H, one would expect also that the C/S ratio also would be subchondritic. Thus, we infer that the major volatile ratios of the BSE record accretion that began during the major early differentiation events of the young Earth as well as addition of a late veneer.

Additional Considerations

The simple model considered here obviously omits many important processes affecting volatiles in the early Earth. For example, the highly dynamic and chaotic processes of accretion, magma ocean formation, degassing, core segregation may not be well-approximated by a simple single stage whole-mantle magma ocean (Tucker and Mukhopahdyay, 2014; Rubie et al. 2015). We also have not considered the possible influence of magma ocean crystallization on fractionation of major volatiles in the non-metallic Earth (Elkins-Tanton, 2008). Preferential storage of H in nominally anhydrous silicates could reduce the C/H ratio of the protomantle and thereby further reduce C/H. On the other hand, enhanced C storage in the crystallized mantle owing to a carbon

pump mechanism (Hirschmann, 2012; Dasgupta et al. 2013) could limit or even reverse this C/H fractionation. It would also possibly minimize the influence of atmospheric loss on the C/S ratio and allow such loss to increase C/N more than loss of a magma ocean atmosphere. These more complex scenarios are all deserving of further investigation.

The calculated atmospheres generated above magma oceans neglect the low temperature processes that occur once those atmospheres cool, including precipitation of a liquid ocean and draw down of CO_2 by weathering (Sleep and Zahnle, 2001; Zahnle et al. 2007; Elkins-Tanton, 2008). These would leave an atmosphere rich in nitrogen, which, if subsequently lost to space, could increase the C/N ratio of the non-metallic Earth. Although loss of all the nitrogen expelled by a magma ocean would not account for the superchondritic C/N ratio of the BSE if significant volatiles are sequestered in the core, as the fraction of N possibly degassed to the atmosphere is less than the fraction of C in the core for nearly all modeled conditions (Fig. 6), magma ocean crystallization could increase atmospheric N_2 to allow such late loss to create a high BSE C/N. In this case, either significant C would have to be retained during magma ocean crystallization (Hirschmann, 2012) or be held in near-surface weathering products.

IMPLICATIONS

The major volatile ratios, C/H, C/N, and C/S, of the BSE are central to understanding of the delivery and processing of the essential ingredients for Earth's climate and habitability. Successful scenarios for accounting for Earth's volatile inventory are best evaluated by their implications for all 3 of these ratios, rather than one or two in isolation. The low C/H ratio of the BSE is a strong signature of events that precede the late veneer and any late volatile additions may have modulated this ratio from formerly more extreme values. The relative contributions of core formation and atmospheric loss to this ratio remain underconstrained, but a more prominent

role of loss of C to space seems less likely in light of superchondritic C/N and nearly chondritic C/S ratios. The high C/N ratio of the BSE could not be a result of core formation and because core formation should leave behind a non-metallic Earth with a very low C/N ratio, may not be tenable from the combination of core formation and subsequent atmospheric blow-off. It seems likely that C/N fractionation on planetesimals and other precursor bodies is needed (Bergin et al. 2015). The nearly chondritic C/S ratio of the BSE likely reflects significant C and S depletion during initial differentiation of the Earth, followed by restoration of the non-metallic Earth C and S budgets either by late accretion of materials with C/S ratios similar to chondrites or by late removal of a S-rich matte to the core (e.g., O'Neill, 1991). The relatively low S content of the BSE is a plausible constraint on the BSE C content, about which there has been significant previous disagreement. The largest C contents previously invoked for the BSE (e.g., Marty, 2012) correspond to superchondritic C/S ratios of nearly 3 and these seem unlikely, as there are few processes that can raise the C/S ratio of the non-metallic Earth above chondritic, with the possible exception of late segregation to the core of a S-rich liquid.

.

Acknowledgements This work benefitted from conversations with many people, including Ted Bergin, Geoff Blake, Fred Ciesla, Jackie Li, Alex Halliday, Bernard Marty, Sujoy Mukhopadhyay, and Sarah Stewart. The comments of Bernard Marty, an anonymous referee, and Associate Editor Tracy Rushmer are appreciated. I gratefully acknowledge support by grants from NASA (NNX11AG64G) and NSF (AST1344133, EAR1426772).

REFERENCES

Ahrens, T.J. (1993) Impact erosion of terrestrial planetary-atmospheres. Annual Review of Earth and Planetary Sciences, 21, 525-555.

699 Albarede, F. (2009) Volatile accretion history of the terrestrial planets and dynamic implications.
700 Nature, 461, 1227-1233.

701 Albarede, F., Ballhaus, C., Blichert-Toft, J., Lee, C.-T., Marty, B., Moynier, F., and Yin, Q.-Z.
702 (2013) Asteroidal impacts and the origin of terrestrial and lunar volatiles. Icarus, 222, 44-
703 52.

704 Alexander, C.M.O.D., Bowden, R., Fogel, M.L., Howard, K.T., Herd, C.D.K., and Nittler, L.R.
705 (2012) The Provenances of Asteroids, and Their Contributions to the Volatile Inventories
706 of the Terrestrial Planets. Science, 337, 721-723.

707 Alexander, C.M.O.D., Howard, K.T., Bowden, R., and Fogel, M.L. (2013) The classification of
708 CM and CR chondrites using bulk H, C and N abundances and isotopic compositions.
709 Geochimica et Cosmochimica Acta, 123, 244-260.

710 Altwegg, K., Balsiger, H., Bar-Nun, A., Berthelier, J.J., Bieler, A., Bochsler, P., Briois, C.,
711 Calmonte, U., Combi, M., De Keyser, J., Eberhardt, P., Fiethe, B., Fuselier, S., Gasc, S.,
712 Gombosi, T.I., Hansen, K.C., Haessig, M., Jaeckel, A., Kopp, E., Korth, A., Leroy, L.,
713 Mall, U., Marty, B., Mousis, O., Neefs, E., Owen, T., Reme, H., Rubin, M., Semon, T.,
714 Tzou, C.Y., Waite, H., and Wurz, P. (2015) 67P/Churyumov-Gerasimenko, a Jupiter
715 family comet with a high D/H ratio. Science, 347, 1261952.

716 Ardia, P., Hirschmann, M.M., Withers, A.C., and Stanley, B.D. (2013) Solubility of CH_4 in a
717 synthetic basaltic melt, with applications to atmosphere-magma ocean-core partitioning
718 of volatiles and to the evolution of the Martian atmosphere. Geochimica et
719 Cosmochimica Acta, 114, 52-71.

720 Arevalo, R., Jr., McDonough, W.F., and Luong, M. (2009) The K/U ratio of the silicate Earth:

721 Insights into mantle composition, structure and thermal evolution. Earth and Planetary
722 Science Letters, 278, 361-369.

723 Armstrong, L.S., Hirschmann, M.M., Stanley, B.D., Falksen, E., and Jacobsen, S.D. (2015)
724 Speciation and solubility of reduced C-O-H-N volatiles in basaltic melt: Implications for
725 volcanism, atmospheric evolution, and deep volatile cycles in the terrestrial planets.
726 Geochimica et Cosmochimica Acta,. doi: http://dx.doi.org/10.1016/j.gca.2015.07.007

727 Aubaud, C., Pineau, F., Jambon, A., and Javoy, M. (2004) Kinetic disequilibrium of C, He, Ar
728 and carbon isotopes during degassing of mid-ocean ridge basalts. Earth and Planetary
729 Science Letters, 222, 391-406.

730 Aubaud, C., Pineau, F., Hekinian, R., and Javoy, M. (2005) Degassing of CO_2 and H_2O in
731 submarine lavas from the Society hotspot. Earth and Planetary Science Letters, 235, 511-
732 527.

733 Aubaud, C., Pineau, F., Hekinian, R., and Javoy, M. (2006) Carbon and hydrogen isotope
734 constraints on degassing of CO_2 and H_2O in submarine lavas from the Pitcairn hotspot
735 (South Pacific). Geophysical Research Letters, 33, L02308.

736 Ballhaus, C., Laurenz, V., Muenker, C., Fonseca, R.O.C., Albarede, F., Rohrbach, A., Lagos, M.,
737 Schmidt, M.W., Jochum, K.-P., Stoll, B., Weis, U., and Helmy, H.M. (2013) The U/Pb
738 ratio of the Earth's mantle-A signature of late volatile addition. Earth and Planetary
739 Science Letters, 362, 237-245.

740 Barry P.H., Hilton, D.R. Füri, E. Halldorsson, S.A. Grönvold, K. (2014) Carbon isotope and
741 abundance systematics of Icelandic geothermal gases, fluids, and subglacial basalts with
742 implications for mantle plume-related CO_2 fluxes. Geochim. Cosmochim. Acta 134 74-

743 99.

744 Bergin, E.A., Blake, G.A., Ciesla, F., Hirschmann, M.M., and Li, J. (2015) Tracing the
745 ingredients for a habitable Earth from interstellar space through planet formation.
746 Proceedings of the National Academy of Sciences, 112, 8965-8970..

747 Boujibar, A., Andrault, D., Bouhifd, M.A., Bolfan-Casanova, N., Devidal, J.-L., and Trcera, N.
748 (2014) Metal-silicate partitioning of sulphur, new experimental and thermodynamic
749 constraints on planetary accretion. Earth and Planetary Science Letters, 391, 42-54.

750 Brooker, R.A., Kohn, S.C., Holloway, J.R., and McMillan, P.F. (2001) Structural controls on the
751 solubility of CO_2 in silicate melts Part I: bulk solubility data. Chemical Geology, 174,
752 225-239.

753 Bureau, H., Metrich, N., Pineau, F., and Semet, M.P. (1998) Magma-conduit interaction at Piton
754 de la Fournaise volcano (Reunion Island): a melt and fluid inclusion study. Journal of
755 Volcanology and Geothermal Research, 84, 39-60.

756 Canfield, D.E. (2004) The evolution of the Earth surface sulfur reservoir. American Journal of
757 Science, 304, 839-861.

758 Cartigny, P., Jendrzejewski, N., Pineau, F., Petit, E., and Javoy, M. (2001) Volatile (C, N, Ar)
759 variability in MORB and the respective roles of mantle source heterogeneity and
760 degassing: the case of the Southwest Indian Ridge. Earth and Planetary Science Letters,
761 194, 241-257.

762 Cartigny, P., Pineau, F., Aubaud, C., and Javoy, M. (2008) Towards a consistent mantle carbon
763 flux estimate: Insights from volatile systematics (H_2O/Ce, delta D, CO_2/Nb) in the North
764 Atlantic mantle (14 degrees N and 34 degrees N). Earth and Planetary Science Letters,

265, 672-685.

Chi, H., Dasgupta, R., Duncan, M.S., and Shimizu, N. (2014) Partitioning of carbon between Fe-rich alloy melt and silicate melt in a magma ocean - Implications for the abundance and origin of volatiles in Earth, Mars, and the Moon. Geochimica et Cosmochimica Acta, 139, 441-471.

Dahl, T.W., and Stevenson, D.J. (2010) Turbulent mixing of metal and silicate during planet accretion - And interpretation of the Hf-W chronometer. Earth and Planetary Science Letters, 295, 177-186.

Dasgupta, R., and Walker, D. (2008) Carbon solubility in core melts in a shallow magma ocean environment and distribution of carbon between the Earth's core and the mantle. Geochimica et Cosmochimica Acta, 72, 4627-4641.

Dasgupta, R., Hirschmann, M.M. and Smith, N.D. (2007) High pressure partial melting experiments of peridotite + CO_2 and genesis of alkalic ocean island basalts. Journal of Petrology 48, 2093-2124.

Dasgupta, R., Buono, A., Whelan, G., and Walker, D. (2009) High-pressure melting relations in Fe-C-S systems: Implications for formation, evolution, and structure of metallic cores in planetary bodies. Geochimica et Cosmochimica Acta, 73, 6678-6691.

Dasgupta, R., Chi, H., Shimizu, N., Buono, A.S., and Walker, D. (2013) Carbon solution and partitioning between metallic and silicate melts in a shallow magma ocean: Implications for the origin and distribution of terrestrial carbon. Geochimica et Cosmochimica Acta, 102, 191-212.

de Niem, D., Kuehrt, E., Morbidelli, A., and Motschmann, U. (2012) Atmospheric erosion and

787 replenishment induced by impacts upon the Earth and Mars during a heavy bombardment.
788 Icarus, 221, 495-507.

789 Deguen, R., Landeau, M., and Olson, P. (2014) Turbulent metal-silicate mixing, fragmentation,
790 and equilibration in magma oceans. Earth and Planetary Science Letters, 391, 274-287.

791 Dixon, J.E., and Clague, D.A. (2001) Volatiles in basaltic glasses from Loihi seamount, Hawaii:
792 Evidence for a relatively dry plume component. Journal of Petrology, 42, 627-654.

793 Dixon, J.E., Clague, D.A., Wallace, P., and Poreda, R. (1997) Volatiles in alkali basalts from the
794 North Arch volcanic field, Hawaii: Extensive degassing of deep submarine-erupted alkali
795 series lavas. 38 911-939.

796 Downes, H., Abernethy, F.A.J., Smith, C.L., Ross, A.J., Verchovsky, A.B., Grady, M.M.,
797 Jenniskens, P., and Shaddad, M.H. (2015) Isotopic composition of carbon and nitrogen in
798 ureilitic fragments of the Almahata Sitta meteorite. Meteoritics & Planetary Science, 50,
799 255-272.

800 Drake, M.J., and Righter, K. (2002) Determining the composition of the Earth. Nature, 416, 39-
801 44.

802 Elkins-Tanton, L.T. (2008) Linked magma ocean solidification and atmospheric growth for Earth
803 and Mars. Earth and Planetary Science Letters, 271, 181-191.

804 Frost, D.J., Mann, U., Asahara, Y., and Rubie, D.C. (2008) The redox state of the mantle during
805 and just after core formation. Philosophical Transactions of the Royal Society a-
806 Mathematical Physical and Engineering Sciences, 366, 4315-4337.

807 Gaetani, G.A., O'Leary, J.A., Shimizu, N., Bucholz, C.E., and Newville, M. (2012) Rapid
808 reequilibration of H_2O and oxygen fugacity in olivine-hosted melt inclusions. Geology,

40, 915-918.

Genda, H., and Abe, Y. (2005) Enhanced atmospheric loss on protoplanets at the giant impact phase in the presence of oceans. Nature, 433, 842-844.

Gibson E.K., and Yanai, K. (1979) Total carbon and sulfur abundances in antarctic meteorites. Proceedings of the Lunar and Planetary Science Conference, 10, 1045-1051.

Goldblatt, C., Claire, M.W., Lenton, T.M., Matthews, A.J., Watson, A.J., and Zahnle, K.J. (2009) Nitrogen-enhanced greenhouse warming on early Earth. Nature Geoscience, 2, 891-896.

Grady, M.M., Wright, I.P., Swart, P.K., and Pillinger, C.T. (1985) The carbon and nitrogen isotopic composition of ureilites - implications for their genesis. Geochimica et Cosmochimica Acta, 49, 903-915.

Grady, M.M., Wright, I.P., Carr, L.P., and Pillinger, C.T. (1986) Compositional differences in enstatite chondrites based on carbon and nitrogen stable isotope measurements. Geochimica et Cosmochimica Acta, 50, 2799-2813.

Halliday, A.N. (2013) The origins of volatiles in the terrestrial planets. Geochimica et Cosmochimica Acta, 105, 146-171.

Hamano, K., Abe, Y., and Genda, H. (2013) Emergence of two types of terrestrial planet on solidification of magma ocean. Nature, 497, 607-611.

Hashimoto, G.L., Abe, Y., and Sugita, S. (2007) The chemical composition of the early terrestrial atmosphere: Formation of a reducing atmosphere from CI-like material. Journal of Geophysical Research-Planets, 112, E05010.

Hayes, J.M., and Waldbauer, J.R. (2006) The carbon cycle and associated redox processes

831 through time. Philosophical Transactions of the Royal Society B-Biological Sciences,
832 361, 931-950.

833 Helo, C., Longpre, M.A., Shimizu, N., Clague, D.A., and Stix, J. (2011) Explosive eruptions at
834 mid-ocean ridges driven by CO_2-rich magmas. Nature Geoscience, 4, 260-263.

835 Hilton, D.R., McMurtry, G.M., and Goff, F. (1998) Large variations in vent fluid $CO_2/^3He$ ratios
836 signal rapid changes in magma chemistry at Loihi seamount, Hawaii. Nature, 396, 359-
837 362.

838 Hirschmann, M.M. (2006) Water, melting, and the deep Earth H_2O cycle. Annual Review of
839 Earth and Planetary Sciences, 34, 629-653.

840 Hirschmann, M.M. (2012) Magma ocean influence on early atmosphere mass and composition.
841 Earth and Planetary Science Letters, 341, 48-57.

842 Hirschmann, M.M., and Dasgupta, R. (2009) The H/C ratios of Earths near-surface and deep
843 reservoirs, and consequences for deep Earth volatile cycles. Chemical Geology, 262, 4-16.

844 Hirschmann, M.M., Withers, A.C., Ardia, P., and Foley, N.T. (2012) Solubility of molecular
845 hydrogen in silicate melts and consequences for volatile evolution of terrestrial planets.
846 Earth and Planetary Science Letters, 345, 38-48.

847 Hofmann, A. (1997) Mantle geochemistry: The message from oceanic volcanism. Nature, 385,
848 219-229.

849 Holloway, J.R., Pan, V., and Gudmundsson, G. (1992) High-pressure fluid-absent melting
850 experiments in the presence of graphite - oxygen fugacity, ferric ferrous ratio and
851 dissolved CO_2. European Journal of Mineralogy, 4, 105-114.

852 Jacobson, S.A., Morbidelli, A., Raymond, S.N., O'Brien, D.P., Walsh, K.J., and Rubie, D.C.

(2014) Highly siderophile elements in Earth's mantle as a clock for the Moon-forming impact. Nature, 508, 84-87.

Jarosewich, E. (2006) Chemical analyses of meteorites at the Smithsonian Institution: An update. Meteoritics & Planetary Science, 41, 1381-1382.

Javoy, M., and Pineau, F. (1991) The volatiles record of a popping rock from the mid-atlantic ridge at 14-degrees N - chemical and isotopic composition of gas trapped in the vesicles. Earth and Planetary Science Letters, 107, 598-611.

Javoy, M., Kaminski, E., Guyot, F., Andrault, D., Sanloup, C., Moreira, M., Labrosse, S., Jambon, A., Agrinier, P., Davaille, A., and Jaupart, C. (2010) The chemical composition of the Earth: Enstatite chondrite models. Earth and Planetary Science Letters, 293, 259-268.

Kadik, A.A., Kurovskaya, N.A., Ignat'ev, Y.A., Kononkova, N.N., Koltashev, V.V., and Plotnichenko, V.G. (2011) Influence of oxygen fugacity on the solubility of nitrogen, carbon, and hydrogen in FeO-Na_2O-SiO_2-Al_2O_3 melts in equilibrium with metallic iron at 1.5 GPa and 1400 degrees C. Geochemistry International, 49, 429-438.

Kerridge, J.F. (1985) Carbon, hydrogen and nitrogen in carbonaceous chondrites - abundances and isotopic compositions in bulk samples. Geochimica et Cosmochimica Acta, 49, 1707-1714.

Koleszar, A.M., Saal, A.E., Hauri, E.H., Nagle, A.N., Liang, Y., and Kurz, M.D. (2009) The volatile contents of the Galapagos plume; evidence for H_2O and F open system behavior in melt inclusions. Earth and Planetary Science Letters, 287, 442-452.

Kuramoto, K. (1997) Accretion, core formation, H and C evolution of the Earth and Mars.

875 Physics of the Earth and Planetary Interiors, 100, 3-20.

876 Kuramoto, K., and Matsui, T. (1996) Partitioning of H and C between the mantle and core during
877 the core formation in the Earth: Its implications for the atmospheric evolution and redox
878 state of early mantle. Journal of Geophysical Research-Planets, 101, 14909-14932.

879 Libourel, G., Marty, B., and Humbert, F. (2003) Nitrogen solubility in basaltic melt. Part I.
880 Effect of oxygen fugacity. Geochimica et Cosmochimica Acta, 67, 4123-4135.

881 Marty, B. (2012) The origins and concentrations of water, carbon, nitrogen and noble gases on
882 Earth. Earth and Planetary Science Letters, 313, 56-66.

883 Marty, B., and Dauphas, N. (2003) The nitrogen record of crust-mantle interaction and mantle
884 convection from Archean to present. Earth and Planetary Science Letters, 206, 397-410.

885 Marty, B., and Zimmermann, L. (1999) Volatiles (He, C, N, Ar) in mid-ocean ridge basalts:
886 Assesment of shallow-level fractionation and characterization of source composition.
887 Geochimica et Cosmochimica Acta, 63, 3619-3633.

888 McDonough, W.F., and Sun, S.S. (1995) The composition of the Earth. Chemical Geology, 120,
889 223-253.

890 McGovern, P.J., and Schubert, G. (1989) Thermal evolution of the earth - effects of volatile
891 exchange between atmosphere and interior. Earth and Planetary Science Letters, 96, 27-
892 37.

893 Melosh, H.J., and Vickery, A.M. (1989) Impact erosion of the primordial atmosphere of Mars.
894 Nature, 338, 487-489.

895 Moore, C.B., and Lewis, C.F. (1966) The distribution of total carbon content in enstatite
896 chondrites. Earth and Planetary Science Letters, 1, 376-378.

897 Moore, G., Vennemann, T., and Carmichael, I.S.E. (1998) An empirical model for the solubility
898 of H_2O in magmas to 3 kilobars. American Mineralogist, 83, 36-42.

899 Morgan, J.W. (1986) Ultramafic xenoliths - clues to Earths late accretionary history. Journal of
900 Geophysical Research-Solid Earth and Planets, 91, 2375-2387.

901 Mysen, B.O., and Fogel, M.L. (2010) Nitrogen and hydrogen isotope compositions and solubility
902 in silicate melts in equilibrium with reduced (N plus H)-bearing fluids at high pressure
903 and temperature: Effects of melt structure. American Mineralogist, 95, 987-999.

904 O'Brien, D.P., Walsh, K.J., Morbidelli, A., Raymond, S.N., and Mandell, A.M. (2014) Water
905 delivery and giant impacts in the 'Grand Tack' scenario. Icarus, 239, 74-84.

906 O'Neill, H.S. (1991) The origin of the Moon and the early history of the Earth – a chemical
907 model. 2. The Earth. Geochimica et Cosmochimica Acta 55, 1159-1172.

908 O'Neill, H.S.C., and Mavrogenes, J.A. (2002) The sulfide capacity and the sulfur content at
909 sulfide saturation of silicate melts at 1400 degrees C and 1 bar. Journal of Petrology, 43,
910 1049-1087.

911 Okuchi, T. (1997) Hydrogen partitioning into molten iron at high pressure: Implications for
912 Earth's core. Science, 278, 1781-1784.

913 Paonita, A., and Martelli, M. (2007) A new view of the He-Ar-CO_2 degassing at mid-ocean
914 ridges: Homogeneous composition of magmas from the upper mantle. Geochemical et
915 Cosmochimica Acta, 71, 1747-1763.

916 Pan, V., Holloway, J.R., and Hervig, R.L. (1991) The pressure and temperature-dependence of
917 carbon-dioxide solubility in tholeiitic basalt melts. Geochimica et Cosmochimica Acta,
918 55, 1587-1595.

Pearson, V.K., Sephton, M.A., Franchi, I.A., Gibson, J.M., and Gilmour, I. (2006) Carbon and nitrogen in carbonaceous chondrites: Elemental abundances and stable isotopic compositions. Meteoritics and Planetary Science, 41, 1899-1918.

Raymond, S.N., Quinn, T., and Lunine, J.I. (2007) High-resolution simulations of the final assembly of earth-like planets. 2. Water delivery and planetary habitability. Astrobiology, 7, 66-84.

Robert, F. (2003) The D/H ratio in chondrites. Space Science Reviews, 106, 87-101.

Robert, F. and Epstein, S. (2002) The concentration and isotopic composition of hydrogen, carbon and nitrogen in carbonaceous meteorites. Geochimica et Cosmochimica Acta, 46, 81-95.

Rosenthal, A., Hauri, E.H., and Hirschmann, M.M. (2015) Experimental determination of C, F, and H partitioning between mantle minerals and carbonated basalt, CO_2/Ba and CO_2/Nb systematics of partial melting, and the CO_2 contents of basaltic source regions. Earth and Planetary Science Letters, 412, 77-87.

Roskosz, M., Bouhifd, M.A., Jephcoat, A.P., Marty, B., and Mysen, B.O. (2013) Nitrogen solubility in molten metal and silicate at high pressure and temperature. Geochimica et Cosmochimica Acta, 121, 15-28.

Rubie, D.C., Frost, D.J., Mann, U., Asahara, Y., Nimmo, F., Tsuno, K., Kegler, P., Holzheid, A., and Palme, H. (2011) Heterogeneous accretion, composition and core-mantle differentiation of the Earth. Earth and Planetary Science Letters, 301, 31-42.

Rubie, D.C., Jacobson, S.A., Morbidelli, A., O'Brien, D.P., Young, E.D., de Vries, J., Nimmo, F., Palme, H., and Frost, D.J. (2015) Accretion and differentiation of the terrestrial planets

941 with implications for the compositions of early-formed Solar System bodies and
942 accretion of water. Icarus, 248, 89-108.

943 Rudge, J.F., Kleine, T., and Bourdon, B. (2010) Broad bounds on Earth's accretion and core
944 formation constrained by geochemical models. Nature Geoscience, 3, 439-443.

945 Saal, A.E., Hauri, E.H., Langmuir, C.H., and Perfit, M.R. (2002) Vapour undersaturation in
946 primitive mid-ocean-ridge basalt and the volatile content of Earth's upper mantle. Nature,
947 419, 451-455.

948 Salters, V.J.M., and Stracke, A. (2004) Composition of the depleted mantle. Geochemistry
949 Geophysics Geosystems, 5, Q05004.

950 Schaefer, L., and Fegley, B., Jr. (2007) Outgassing of ordinary chondritic material and some of
951 its implications for the chemistry of asteroids, planets, and satellites. Icarus, 186, 462-483.

952 Schaefer, L., and Fegley, B., Jr. (2010) Chemistry of atmospheres formed during accretion of the
953 Earth and other terrestrial planets. Icarus, 208, 438-448.

954 Schlichting, H.E., Sari, R., and Yalinewich, A. (2015) Atmospheric mass loss during planet
955 formation: The importance of planetesimal impacts. Icarus, 247, 81-94.

956 Sedwick, P.N. McMurtry, G.M., Hilton, D.R., Goff, F. (1993) Carbon dioxide and helium in
957 hydrothermal fluids from Loihi seamount, Hawaii, USA: Temporal variability and
958 implications for the release of mantle volatiles. Geochimica et Cosmochimica Acta, 58,
959 1219-1227.

960 Shaw, A.M., Behn, M.D., Humphris, S.E., Sohn, R.A., and Gregg, P.M. (2010) Deep pooling of
961 low degree melts and volatile fluxes at the 85 degrees E segment of the Gakkel Ridge:
962 Evidence from olivine-hosted melt inclusions and glasses. Earth and Planetary Science

Letters, 289, 311-322.

Siebert, J., Badro, J., Antonangeli, D., and Ryerson, F.J. (2013) Terrestrial accretion under oxidizing conditions. Science, 339, 1194-1197.

Sleep, N.H., and Zahnle, K. (2001) Carbon dioxide cycling and implications for climate on ancient Earth. Journal of Geophysical Research-Planets, 106, 1373-1399.

Stanley, B.D., Hirschmann, M.M., and Withers, A.C. (2011) CO_2 solubility in Martian basalts and Martian atmospheric evolution. Geochimica et Cosmochimica Acta, 75, 5987-6003.

Stanley, B.D., Hirschmann, M.M., and Withers, A.C. (2014) Solubility of C-O-H volatiles in graphite-saturated martian basalts. Geochimica et Cosmochimica Acta, 129, 54-76.

Stixrude, L., de Koker, N., Sun, N., Mookherjee, M., and Karki, B.B. (2009) Thermodynamics of silicate liquids in the deep Earth. Earth and Planetary Science Letters, 278, 226-232.

Stolper, E., and Holloway, J.R. (1988) Experimental-determination of the solubility of carbon-dioxide in molten basalt at low-pressure. Earth and Planetary Science Letters, 87, 397-408.

Trull, T. Nadeau, S., Pineau, F. Polvé, M., and Javoy, M. (1993) C-He systematics in hotspot xenoliths: Implications for mantle carbon contents and carbon recycling. Earth and Planetary Science Letters, 118, 43-64.

Tsuno, K., and Dasgupta, R. (2015) Fe-Ni-Cu-C-S phase relations at high pressures and temperatures - The role of sulfur in carbon storage and diamond stability at mid- to deep-upper mantle. Earth and Planetary Science Letters, 412, 132-142.

Tucker, J.M., and Mukhopadhyay, S. (2014) Evidence for multiple magma ocean outgassing and atmospheric loss episodes from mantle noble gases. Earth and Planetary Science Letters,

393, 254-265.

Wacheul, J.-B., Le Bars, M., Monteux, J., and Aurnou, J.M. (2014) Laboratory experiments on the breakup of liquid metal diapirs. Earth and Planetary Science Letters, 403, 236-245.

Walker, R.J. (2009) Highly siderophile elements in the Earth, Moon and Mars: Update and implications for planetary accretion and differentiation. Chemie Der Erde-Geochemistry, 69, 101-125.

Wang, Z., and Becker, H. (2013) Ratios of S, Se and Te in the silicate Earth require a volatile-rich late veneer. Nature, 499, 328--332.

Wanless, V.D., and Shaw, A.M. (2012) Lower crustal crystallization and melt evolution at mid-ocean ridges. Nature Geoscience, 5, 651-655.

Wanless, V.D., Behn, M.D., Shaw, A.M., and Plank, T. (2014) Variations in melting dynamics and mantle compositions along the Eastern Volcanic Zone of the Gakkel Ridge: insights from olivine-hosted melt inclusions. Contributions to Mineralogy and Petrology, 167, 1005.

Warren, P.H. (2008) A depleted, not ideally chondritic bulk Earth: The explosive-volcanic basalt loss hypothesis. Geochimica et Cosmochimica Acta, 72, 2217-2235.

Warren, P.H. Ulff-Møller, F., Huber, H., Kallemeyn, G.W. (2006) Siderophile geochemistry of ureilites: A record of early stages of planetesimal core formation. Geochimica et Cosmochimica Acta 70, 2104-2126.

Wasson, J.T., and Kallemeyn, G.W. (1988) Compositions of chondrites. Philosophical Transactions of the Royal Society a-Mathematical Physical and Engineering Sciences, 325, 535-544.

1007 Wetzel, D.T., Rutherford, M.J., Jacobsen, S.D. Hauri, E.H. Saal, A.E. (2013) Degassing of
1008 reduced carbon from planetary basalts. Proceedings of the National Academy of Sciences,
1009 110, 8010-8013.

1010 Wood, B.J. (1993) Carbon in the core. Earth and Planetary Science Letters, 117, 593-607.

1011 Wood, B.J., and Halliday, A.N. (2005) Cooling of the Earth and core formation after the giant
1012 impact. Nature, 437, 1345-1348.

1013 Workman, R.K., and Hart, S.R. (2005) Major and trace element composition of the depleted
1014 MORB mantle (DMM). Earth and Planetary Science Letters, 231, 53-72.

1015 Zahnle, K., Arndt, N., Cockell, C., Halliday, A., Nisbet, E., Selsis, F., and Sleep, N.H. (2007)
1016 Emergence of a habitable planet, p. 35-78.

1017 Zhang, Z., and Hirschmann, M.M. (2016) Experimental constraints on mantle sulfide melting up to 8
1018 GPa. American Mineralogist

1019 **Figure Captions**

1020 **Figure 1** Cartoon of a magma ocean equilibrating with an overlying atmosphere and with alloy
1021 as it transits to the core. Equilibrium of a volatile element, *i*, between the silicate and overlying
1022 atmosphere with a partial vapor pressure given by Pi, is controlled by a Henrian solubility
1023 constant, Si, (Eqn. 6). Equilibrium between silicate and alloy as it transits to the core is
1024 approached according to the alloy/silicate partition coefficient, $D_i^{alloy/silicate}$. The proportion of
1025 metal that equilibrates with the volatile-bearing silicate depends on the dynamics of core
1026 segregation as well as the timing of delivery of accreting volatiles relative to that of accreting
1027 metal. Note that the partial pressure of a volatile component in the atmosphere depends on the
1028 solubility constant as well as on the value of $D_i^{alloy/silicate}$. Components that are less soluble and/or

have large values of $D_i^{alloy/silicate}$ will have lower atmospheric partial pressures. Conversely, components that are highly incompatible in silicate and/or low values of $D_i^{alloy/silicate}$ will have comparatively lower concentrations in the core-destined alloy.

Figure 2 C/H ratios of less-degassed oceanic basalts. Data for Oceanic Basalts (OIB) from Loihi (Dixon and Clague, 2001), Galapagos (Fernandina and Santiago) (Koleszar et al. 2009), Pitcairn (Aubaud et al. 2006), Society Islands (Aubaud et al. 2005), Reunion (Bureau et al. 1998). Data for Mid-Ocean Ridge Basalts (MORB) from the Gakkel ridge (Shaw et al. 2010; Wanless et al. 2014), Siqueiros Deep (Saal et al. 2002), Pito Deep (Aubaud et al. 2004), Juan de Fuca ridge and East Pacific Rise (Wanless and Shaw, 2012), North Atlantic popping rocks (Cartigny et al., 2008, using the reconstruction of Hirschmann and Dasgupta, 2009), and Axial Seamount (Helo et al. 2009). Horizontal solid lines are mean values for OIB and MORB, with uncertainties shaded. Horizontal dashed lines are the values inferred by Hirschmann and Dasgupta (2009) based on a subset of the presently available data.

Figure 3 C/H ratio of the BSE (Table 1) compared to values from chondritic meteorites. Carbonaceous chondrite (CI, CO, CM, CV) ratios are averages from the compilation of meteorite falls by Kerridge (1985). Ordinary chondrite ratios are averages of falls from compilation of Jarosewich (2006) and Schaefer and Fegley (2007). For each, the range represents the C/H ratio calculated using only H_2O released at high temperature (H_2O^+) and using all released H_2O (H_2O^+ and H_2O^-). As the latter likely contains some terrestrial contamination (Robert and Epstein, 2002), it overestimates total H. Data for H contents of enstatite chondrites are rare, with only two published concentrations for falls (Abee and Hvittis) from Robert (2003) – because this study lumps high temperature (H_2O^+) and low temperature (H_2O^-), it may overestimate native enstatite

chondrite H_2O. These were combined with C analyses for Abee (Grady et al., 1986) and Hvittis (Moore and Lewis, 1966) to calculate C/H ratios.

Figure 4 C/N ratios of chondritic meteorites compared to the BSE (Bergin et al. 2015). Ratios for different carbonaceous chondrite classes include CI, CM, CO, CV, CK, and CR. Separate values are plotted from the studies of Kerridge (1985); Pearson et al. (2006); and Alexander et al. (2012; 2013) because of strong differences between studies for some groups, most notably the C-poor CO and CV types. Samples from Kerridge (1985) are falls as are 21 of 26 from Pearson et al. (2006), but samples analyzed by Alexander et al. (2012; 2013) are chiefly finds from Antarctica. For ordinary chondrites, the compiled averages for H, L, and LL classes are taken from the compilation of falls from Schaefer and Fegley (2007) and from falls and finds from Bergin et al. (2015). Enstatite (EH, EL) chondrite ratios are from averages of compilations by Grady et al. (1986) and Wasson and Kallemeyn (1988).

Figure 5 C/S ratios of chondritic meteorites compared to the BSE. For the BSE, C is calculated as described in the text, and S is taken to be 225±25 ppm, consistent with Morgan (1986), McDonough and Sun (1995), and Wang and Becker (2014). C/S ratios of carbonaceous chondrites (CI, CM, CO, CV), ordinary chondrite (H, L, LL), and enstatite chondrites (EH, EL) from Wasson and Kallemeyn (1988).

Figure 6 Proportions of major volatiles in the atmosphere and in alloy for an oxidized (IW+1), reduced (IW-2) and very reduced (IW-3.5) differentiating molten planet, calculated from Eqns. 1-7 and the solubility constants and metal/alloy partition coefficients in Table 2. The calculation assumes equilibration between a mass of silicate (volatile proportions not shown) amounting to the current mantle (4×10^{27} g) with variable metal/silicate mass ratios from 0 to 0.5 (alloy mass=0-2 $\times 10^{27}$ g) and an overlying atmosphere. Initial concentrations are C: 4000 ppm, H:

200 ppm, N: 160 ppm, S: 6000 ppm, which give approximately chondritic ratios (C/H=10, C/N=25, C/S=0.667). Atmospheric proportions of S for all cases and of H for oxidized and reduced cases are not evident in figure because they are too close to zero.

Figure 7 Major volatile ratios (C/H, C/N, C/S) of the atmosphere and in alloy for the calculations described in Fig. 6. Solid curves show ratios in the non-metallic Earth (silicate+ atmosphere) after removal of alloy to the core. Dashed curves show ratios in the non-metallic Earth (silicate) after removal of alloy to the core and subsequent loss of the overlying atmosphere. BSE ranges from Table 1.

Figure 8 Comparison of the BSE volatile concentrations, normalized to CI chondrites (Table 1 with model calculations of the non-metallic Earth. BSE composition based on ratios shown in Figs 3, 4, and 5, with the BSE C concentration (90 ppm) derived from the analysis of C/H ratios in undegassed basalts, as described in the text. In these calculations, the original volatile inventory accreted to the Earth is assumed to derive from 1.5% Earth masses of carbonaceous (CI) chondrites, consistent with both geochemical and dynamical models (Drake and Righter, 2002; O'Brien et al. 2014). In each panel, variable amounts of metal, ranging from 0 to 50% of the mass of the non-metallic Earth, equilibrate with the silicate and atmospheric reservoirs of the Earth based on the "reduced" solubilities and partition coefficients from Table 2. In panels B, C, and D, the atmosphere is subsequently lost to space. In panels d and d, a late veneer, in addition to the original volatile inventory, amounting to 0.3% Earth masses (e.g. Walker, 2009) is accreted after closure of the mantle to core formation and any catastrophic atmospheric loss. In panel C, the late veneer has the composition of CI chondrite. In panel D, the late veneer has the composition equal to 20% CI chondrite, 80% ureilite (Table 2). Note that absolute concentrations elements in non-metallic Earth calculations are somewhat arbitrary, as these could

1097 be altered by assuming different amounts (or compositions) of volatile-rich materials accreated
1098 to the Earth. Therefore, it is the (C/H, C/N, C/S) ratios of different elements that are of greatest
1099 interest in the comparisons depicted.

Table 1. Major volatile element ratios in the Bulk Silicate Earth (BSE)		
	BSE	Source
C/H	1.13±0.20	This study: from C/H of basalts
C/H	1.4±0.4	This study: from C/Ba and C/Nb of basalts
C/N	40±8	Bergin et al. 2015
C/S	0.49±0.14	This study

Table 2 Volatile solubilities and partition coefficients used for model calculations			
		Solubility Constants	Partition Coefficients
		S_i (Eqn. 6) (ppm/MPa)	$D_i^{alloy/silicate}$
C	oxidized	1.6	500
	reduced	0.55	1000
	v. reduced	0.22	3000
H	oxidized	*	6.5
	reduced	*	6.5
	v. reduced	5	6.5
N	oxidized	1	20
	reduced	5	20
	v. reduced	50	20
S	oxidized	5000	60
	reduced	5000	60
	v. reduced	5000	60
Sources of solubility constants, S_i, are described in text. Choices of partition coefficients, $D_i^{alloy/silicate}$, are chosen to be consistent with experimental constraints from Chi et al. (2014) and Armstrong et al. (2015) (C), Okuchi (1997), Roskosz et al., 2013 (N), and Boujibar et al. (2014) (S) for shallow mantle (< 10 GPa, <2000 K) conditions. * Moore et al. 1998			

Table 3 Accreted material compositions used for model calculations

	"CI" ppm	Reference	"Ureilite" ppm	Reference
C	35000	(1)	30000	(3)
H	6900	(1)	2000	(4)
N	1500	(1)	30	(3,5)
S	65000	(2)	3000	(6)

(1) Kerridge (1985) (2) from C and C/S ratio (0.54) of Wasson and Kallemeyn (1988) (3) Grady et al (1985) (4) Jarosewich (2006) (5) Downes et al. (2015) (6) Gibson and Yanai (1979)

Figure 1

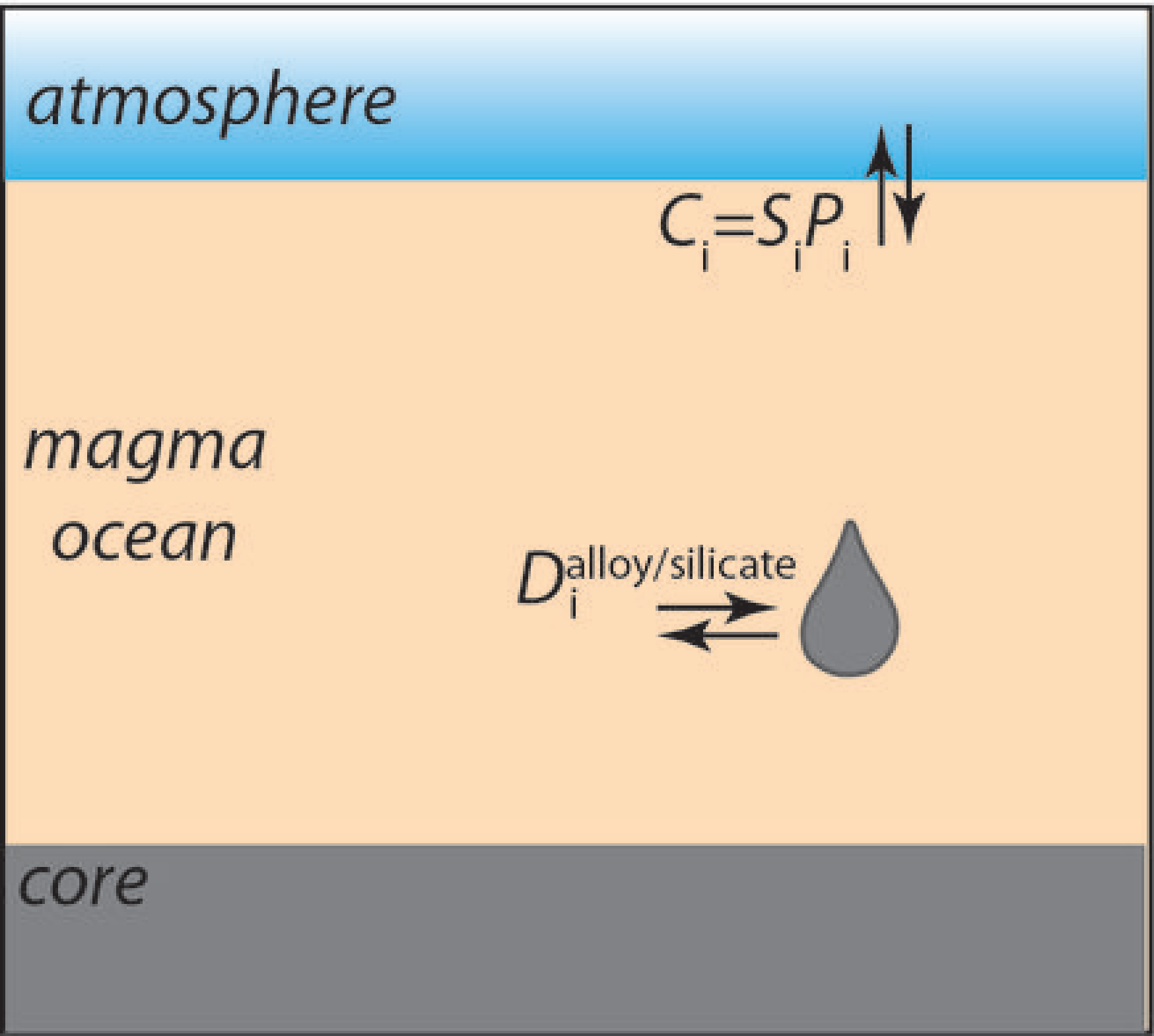

Figure 2

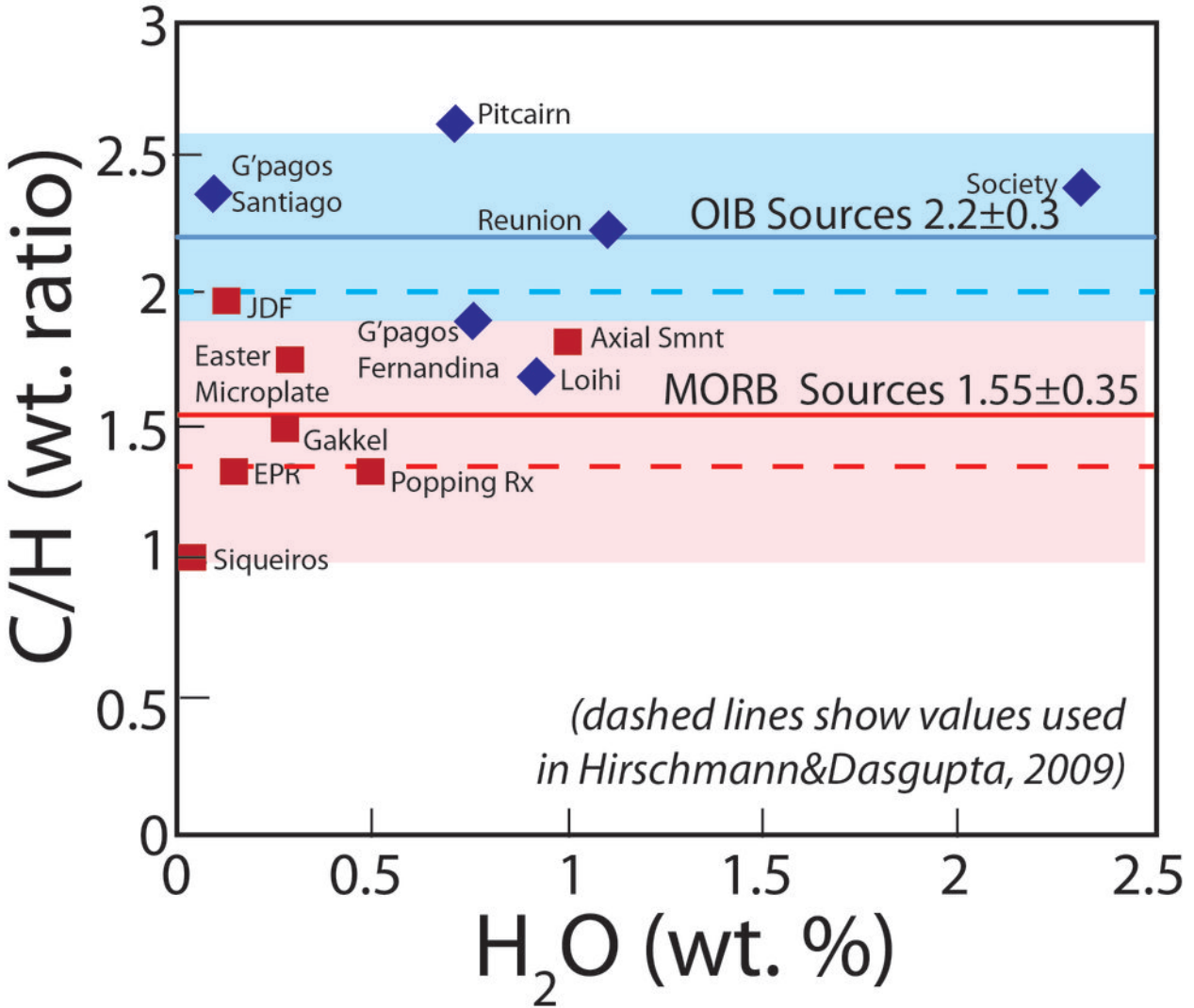
C/H (wt. ratio)
H2O (wt. %)
0
0.5
1
1.5
2
2.5
3
Pitcairn
G'pagos
Santiago
Reunion
Society
OIB Sources 2.2±0.3
JDF
G'pagos
Fernandina
Axial Smnt
Easter
Microplate
Loihi
MORB Sources 1.55±0.35
Gakkel
EPR
Popping Rx
Siqueiros
(dashed lines show values used
in Hirschmann&Dasgupta, 2009)

Figure 3

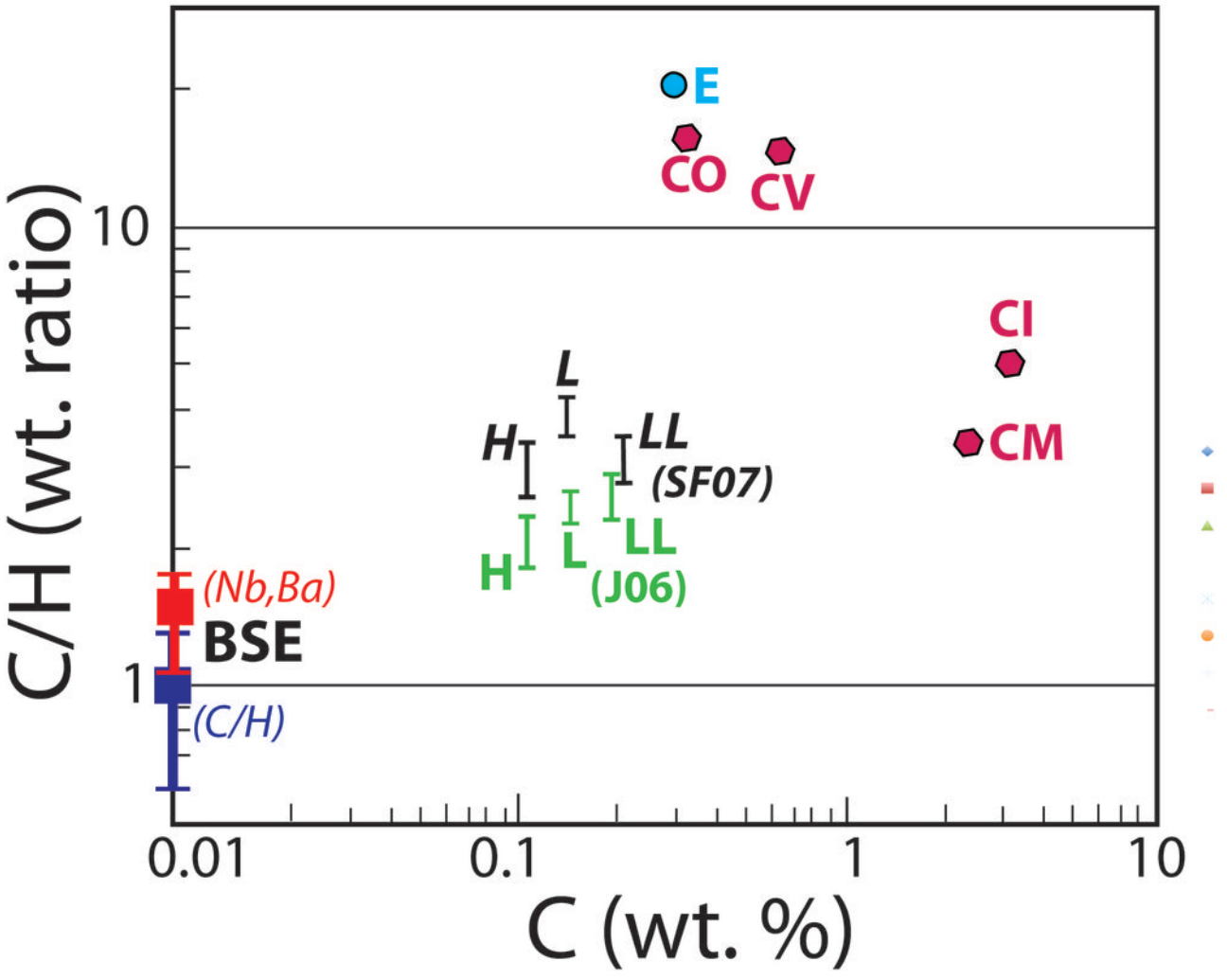
E
CO
CV
CI
CM
L
H
LL
(SF07)
H
L
LL
(J06)
(Nb,Ba)
BSE
(C/H)
10
1
0.01
0.1
1
10
C/H (wt. ratio)
C (wt. %)

Figure 4

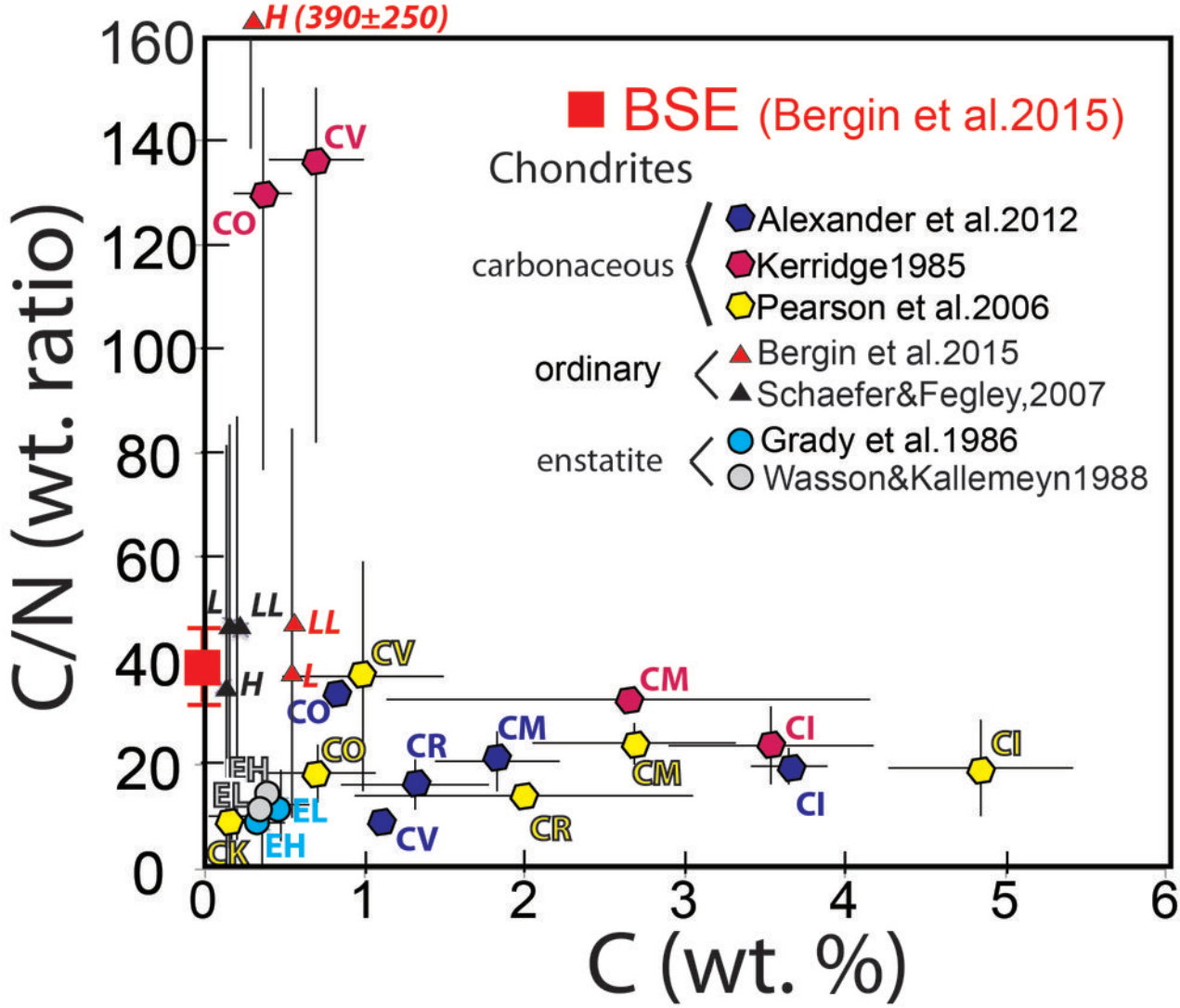
H (390±250)
BSE (Bergin et al.2015)
Chondrites
carbonaceous
Alexander et al.2012
Kerridge1985
Pearson et al.2006
ordinary
Bergin et al.2015
Schaefer&Fegley,2007
enstatite
Grady et al.1986
Wasson&Kallemeyn1988
C/N (wt. ratio)
C (wt. %)
0
20
40
60
80
100
120
140
160
0
1
2
3
4
5
6
CV
CO
CM
CR
CI
CK
EH
EL
L
LL
H

Figure 5

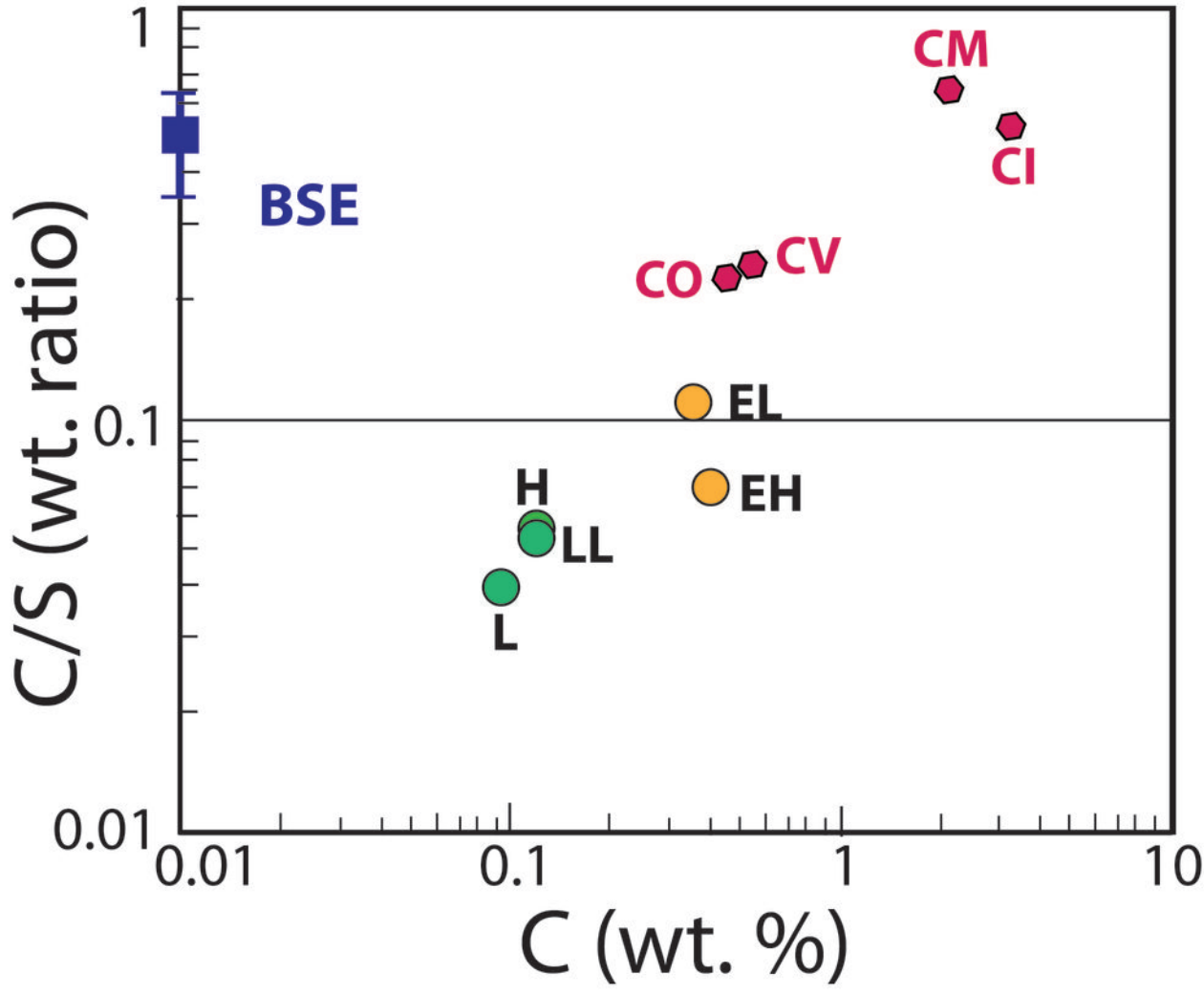

Figure 6

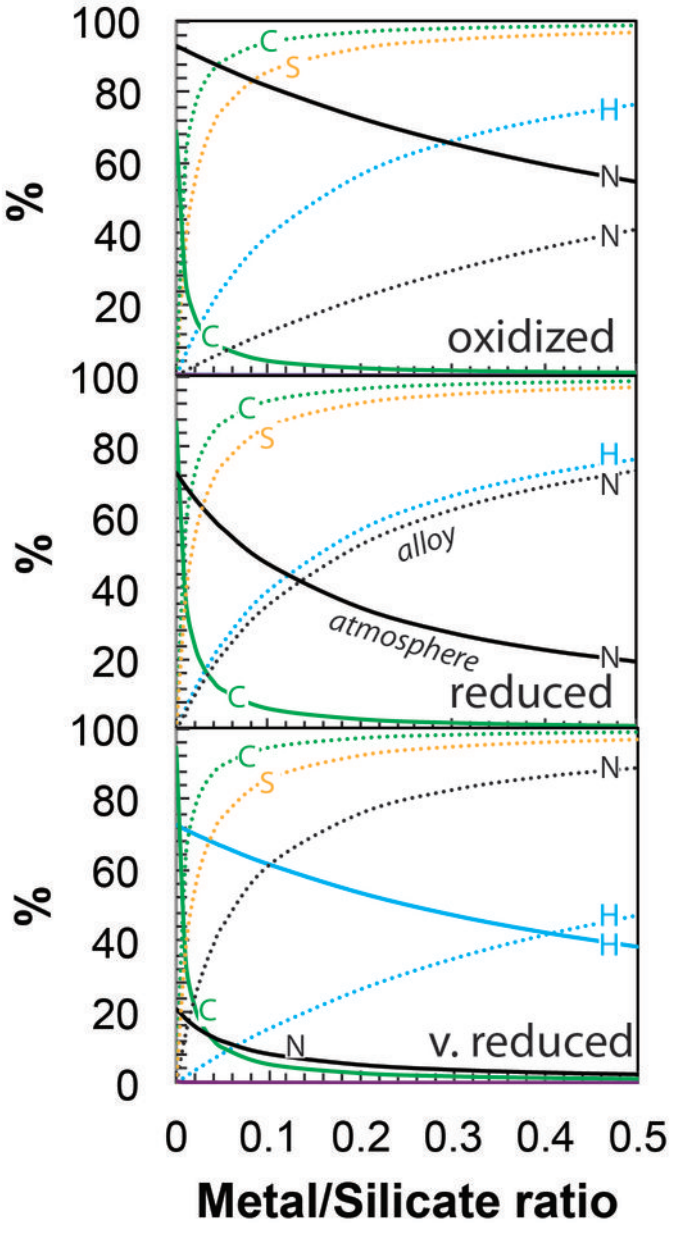
100
80
60
40
20
%
C
S
H
N
N
C
oxidized
100
80
60
40
20
%
C
S
H
N
alloy
atmosphere
N
C
reduced
100
80
60
40
20
0
%
C
S
N
H
H
C
N
v. reduced
0
0.1
0.2
0.3
0.4
0.5
Metal/Silicate ratio

Figure 7

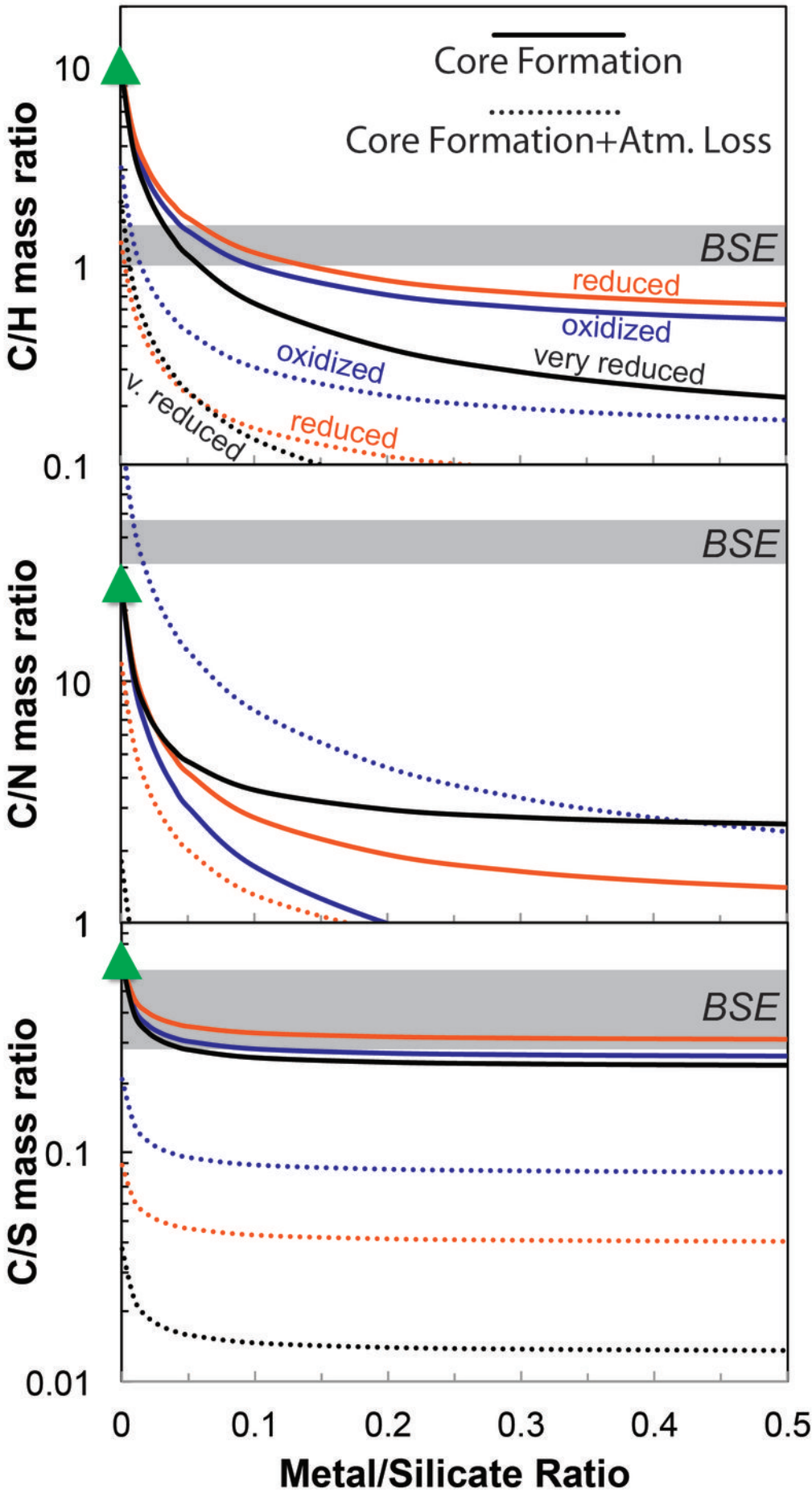
Core Formation
Core Formation+Atm. Loss
BSE
reduced
oxidized
very reduced
oxidized
v. reduced
reduced
C/H mass ratio
10
1
0.1
BSE
C/N mass ratio
10
1
BSE
C/S mass ratio
0.1
0.01
0
0.1
0.2
0.3
0.4
0.5
Metal/Silicate Ratio

Figure 8

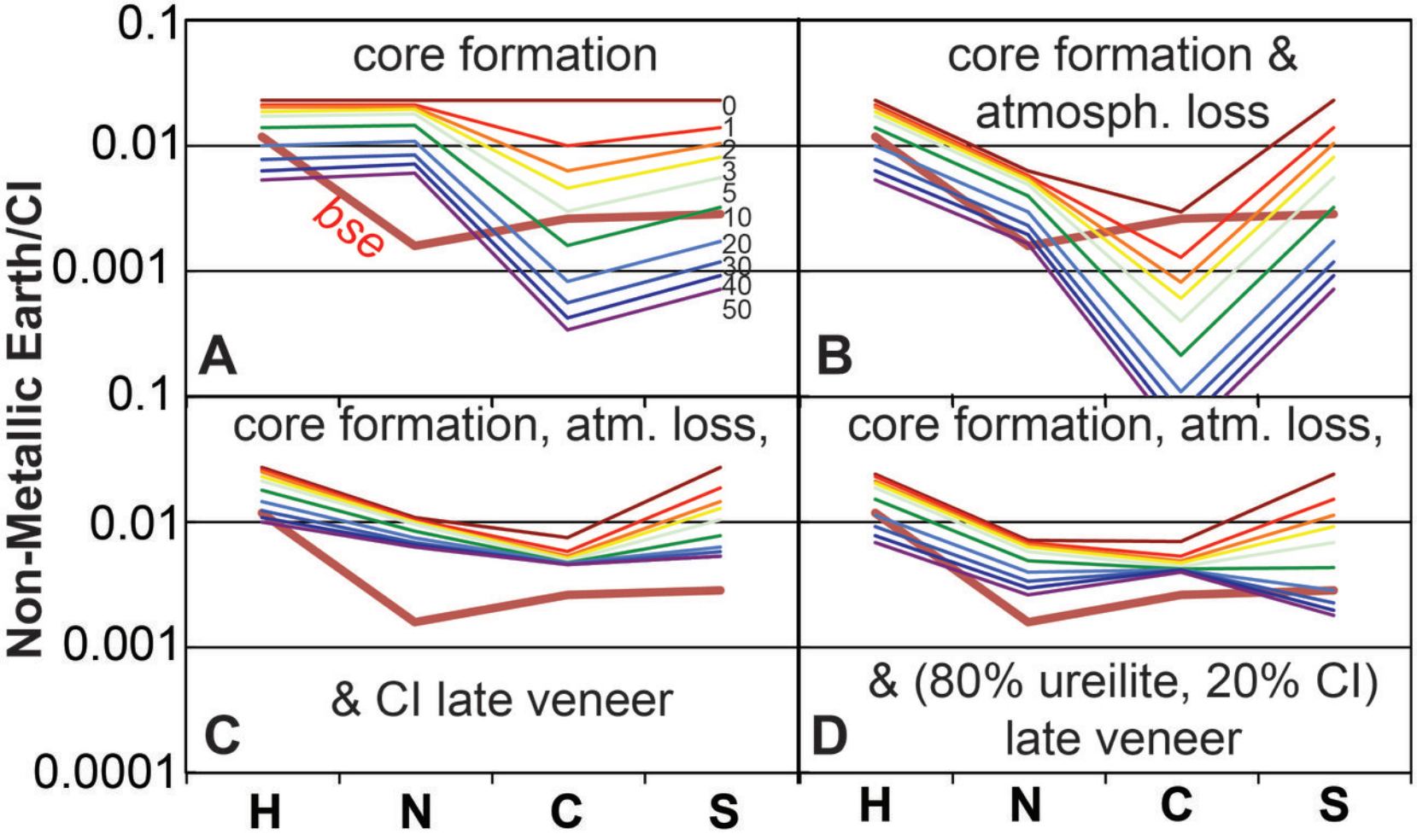
Non-Metallic Earth/CI
0.1
0.01
0.001
0.1
0.01
0.001
0.0001
core formation
bse
0
1
2
3
5
10
20
30
40
50
A
core formation &
atmosph. loss
B
core formation, atm. loss,
& CI late veneer
C
core formation, atm. loss,
& (80% ureilite, 20% CI)
late veneer
D
H
N
C
S
H
N
C
S